

1

AD-A284 562



ARMY RESEARCH LABORATORY



A Technical Demonstration Mobile Profiler System

by James L. Cogan
Battlefield Environment Directorate

ARL-TR-523

August 1994

DTIC
ELECTE
SEP 20 1994
S D

94-30208



94 9 18 111

NOTICES

Disclaimers

The findings in this report are not to be construed as an official Department of the Army position, unless so designated by other authorized documents.

The citation of trade names and names of manufacturers in this report is not to be construed as official Government indorsement or approval of commercial products or services referenced herein.

Destruction Notice

When this document is no longer needed, destroy it by any method that will prevent disclosure of its contents or reconstruction of the document.

DISCLAIMER NOTICE



THIS DOCUMENT IS BEST QUALITY AVAILABLE. THE COPY FURNISHED TO DTIC CONTAINED A SIGNIFICANT NUMBER OF COLOR PAGES WHICH DO NOT REPRODUCE LEGIBLY ON BLACK AND WHITE MICROFICHE.

REPORT DOCUMENTATION PAGE

Form Approved
OMB No. 0704-0188

Public reporting burden for this collection of information is estimated to average 1 hour per response, including the time for reviewing instructions, searching existing data sources, gathering and maintaining the data needed, and completing and reviewing the collection of information. Send comments regarding this burden estimate or any other aspect of this collection of information, including suggestions for reducing this burden, to Washington Headquarters Services, Directorate for Information Operations and Reports, 1215 Jefferson Davis Highway, Suite 1204, Arlington, VA 22202-4302, and to the Office of Management and Budget, Paperwork Reduction Project (0704-0188), Washington, DC 20503.

1. AGENCY USE ONLY (Leave blank)		2. REPORT DATE August 1994	3. REPORT TYPE AND DATES COVERED	
4. TITLE AND SUBTITLE A Technical Demonstration Mobile Profiler System			5. FUNDING NUMBERS	
6. AUTHOR(S) James L. Cogan				
7. PERFORMING ORGANIZATION NAME(S) AND ADDRESS(ES) U.S. Army Research Laboratory Battlefield Environment Directorate ATTN: AMSRL-BE-W White Sands Missile Range, NM 88002-5501			8. PERFORMING ORGANIZATION REPORT NUMBER ARL-TR-523	
9. SPONSORING/MONITORING AGENCY NAME(S) AND ADDRESS(ES) U.S. Army Research Laboratory 2800 Powder Mill Road Adelphi, MD 20783-1145			10. SPONSORING/MONITORING AGENCY REPORT NUMBER ARL-TR-523	
11. SUPPLEMENTARY NOTES				
12a. DISTRIBUTION / AVAILABILITY STATEMENT Approved for public release; distribution is unlimited.			12b. DISTRIBUTION CODE A	
13. ABSTRACT (Maximum 200 words) A near, real time sounding of the atmosphere from the surface to ≥ 30 km over a battlefield may be obtained by combining atmospheric profiles from meteorological (MET), satellite, and ground-based instruments. This type of capability is essential for optimum use of Army resources such as artillery and defense against biological and chemical attack. The technical demonstration (TD) mobile profiler system (MPS) has this capability and plays an important role in a variety of civilian applications, including detailed analysis of MET variables for research and operations over mesoscale areas (regional pollution studies and severe storm forecasting). This report provides a brief description of the TD MPS and the method for merging data from the satellite and ground-based remote sensing systems. Results presented from a month-long field test indicate the ability of the present version of the TD MPS to generate useful atmospheric soundings in the format of an artillery MET message and a variety of other formats and displays. Comparisons made with data from rawinsondes nearly coincident in space and time indicate the level of accuracy of the data. An intercomparison between two rawinsonde systems on site suggest possible errors in the rawinsonde data.				
DTIC QUALITY INSPECTED 7				
14. SUBJECT TERMS mobile profiler, combined soundings, atmospheric soundings			15. NUMBER OF PAGES 55	
			15. PRICE CODE	
17. SECURITY CLASSIFICATION OF REPORT Unclassified	18. SECURITY CLASSIFICATION OF THIS PAGE Unclassified	19. SECURITY CLASSIFICATION OF ABSTRACT Unclassified	20. LIMITATION OF ABSTRACT SAR	

Acknowledgments

The graphics software used to produce the displays of sensor data (figures 2, 4 through 9, 13, and 14) were designed and modified by B. Weber, M. Simon, A. Simon, D. Weurtz, S. King, D. Merritt, and D. Wolfe, of National Oceanic and Atmospheric Administration Environmental Technology Laboratory. These personnel, D. Littell of Army Research Laboratory (ARL), Battlefield Environment Directorate and J. Cogan operated the technical demonstration mobile profiler system (TD MPS). E. Measure of ARL provided charts of ground-based radiometer temperatures versus rawinsonde temperatures from which the relevant figure of this report was derived. D. Littell also provided assistance in the repair and maintenance of the TD MPS.

Accession For	
NTIS CRA&I	<input checked="" type="checkbox"/>
DTIC TAB	<input type="checkbox"/>
Unannounced	<input type="checkbox"/>
Justification	
By	
Distribution/	
Availability Codes	
Dist	Avail and/or Special
A-1	

Contents

Acknowledgments	1
1. Introduction	7
2. System Description	9
3. Combining Method	11
4. Data	15
5. Comparisons	21
6. Potential Problems and Solutions	37
7. Conclusions	49
References	51
Acronyms and Abbreviations	53
Distribution	55

Figures

1. Combined sounding concept. Satellite and ground-based data are merged to form a more accurate sounding for the atmosphere from the surface to the highest satellite sounding level 12
2. Block diagram of the combined sounding program and computation of layer values for input to MET messages. 13
3. Tabular output from the combining software on the TD MPS in the format of the MET-CM artillery MET message 15
4. Time-height display of wind velocity profiles from the 924 MHz radar profiler. Wind arrows of full and half barb represent 10 and 5 m/s, respectively. The site is Claremont, CA (Los Angeles basin). Soundings derived using 15 min of data, and displayed every half hour 17
5. Time-height display of virtual temperature from the RASS. Missing data adjacent to the surface were removed by the quality control routine 18
6. Time-height display of combined wind velocity profiles derived from radar profiler and satellite data 19
7. Virtual temperature (°C) comparison between RASS and rawinsonde. MPSB indicates rawinsonde 23
8. Virtual temperature (°C) comparison between satellite and rawinsonde. 24
9. Virtual temperature (°C) comparison between the combined sounding and rawinsonde 25
10. Wind speed comparison (m/s) between the radar profiler and rawinsonde 26
11. Virtual temperature (°C) comparison between RASS and rawinsonde showing mean and standard deviations on each of three days. The time window varied from 5 to 120 min 29

Figures (continued)

12.	Virtual temperature ($^{\circ}\text{C}$) comparison between combined soundings (RASS and satellite) and rawinsonde showing mean and standard deviations on each of three days. The time window varied from 30 to 180 min	32
13.	Temperature comparison ($^{\circ}\text{C}$) between the ground-based microwave radiometer and rawinsonde. The points shown for the radiometer represent mean values for volumes of atmosphere, as opposed to point values from the rawinsonde	33
14.	Wind velocity display comparing profiles from two rawinsonde systems, Marwin (right) and CLASS (left), using the same sonde. The profiles are offset from one another for clarity of presentation. (good case)	34
15.	Wind velocity display as in figure 10. (poor case)	35
16.	Wind speed comparison (m/s) between the radar profiler and rawinsonde for the period 1300-2000 UT, 11 September 1993	39
17a.	Wind speed comparison (m/s) between the radar profiler and rawinsonde for the 0.1-1.0 km layer	40
17b.	Wind speed comparison (m/s) between the radar profiler and rawinsonde for the 1.0-2.0 km layer	41
17c.	Wind speed comparison (m/s) between the radar profiler and rawinsonde for the 2.0-3.0 km layer	42
17d.	Wind speed comparison (m/s) between the radar profiler and rawinsonde for the 3.0-4.0 km layer	43
18.	Graphical time-height display of wind velocity from rawinsonde measurements for the period of 1300-2000 UT, 11 September 1993	44
19.	Graphical time-height display of wind velocity from radar profiler measurements for the period of figure 16	45
20.	Graphical time-height display of wind velocity from the radar profiler. Five min averages are displayed every 5 min during 2130-2300 UT, 8 September 1993	46

1. Introduction

The Mobile Profiler System (MPS) is being developed to provide field artillery with atmospheric soundings in near, real time. The reduction of refresh time of 2 to 4 hr, using balloon systems such as the Meteorological Data System (MDS), to 15 to 30 min will considerably reduce errors caused by time staleness. [1] Seagraves and McPeck [2] briefly describe the objective system concept. Systems of the type found in technical demonstration (TD) MPS are described in Cogan, [3] Miers et al., [4] their references, Hassel and Hudson, [5] and Strauch et al. [6] This report briefly describes the TD MPS, provides an outline of the combined sounding technique, and presents examples of actual data in a variety of formats. Comparisons with rawinsonde soundings nearly coincident in space and time provide an indication of the accuracy of the system. The usefulness of rawinsondes as a standard is suggested through comparisons of wind velocity soundings from a Marwin and a Cross-chain Loran Atmospheric Sounding System (CLASS) in which the systems received data from the same sonde. The TD MPS project is an ongoing joint effort by the U.S. Army Research Laboratory (ARL), Battlefield Environment Directorate (BED) (lead organization) and the National Oceanic and Atmospheric Administration (NOAA), Environmental Technology Laboratory (ETL), Boulder, CO.

2. System Description

The TD MPS consists of a five beam, phased array, 924 MHz radar profiler for wind velocity; a Radio Acoustic Sounding System (RASS) for virtual temperature (acoustic frequency approximately 2 kHz); a ground-based microwave radiometer for temperature and humidity; a small surface station for temperature, pressure, humidity and wind velocity; and a receiver/processor for acquisition of satellite sounder data for temperature and humidity. The radiometer measures radiance at 51.7, 54.0, 55.3, and 57.0 GHz for temperature, and at frequencies of 20.7 and 31.5 GHz for water vapor and liquid.* It scans five angles from 9 to 90° for temperature, and three angles from 30 to 90° for moisture (effectively five directions because it scans the same two slant path angles at opposite sides of the vertical path). Geopotential heights for the satellite sounding are computed for the standard pressure levels. Wind velocity for the satellite sounding is calculated from gradients of the satellite heights using the geostrophic assumption. Temperature is converted to virtual temperature as required. Pressure versus height is calculated from the sounding data and measured for the lower part of the sounding by a microwave radiometer. As of the preparation of this report, the operational parts of the TD MPS were the radar profiler, the RASS, the surface station, and the satellite receiver/processor. The microwave radiometer was being integrated into the system. A 9-m (30-ft) trailer with shelter houses the components of the TD MPS, except for the radar antenna, the four RASS transducers, the satellite receiver antenna, and the microwave radiometer. The primary processors are an HP 720 for the satellite terminal and an HP 735 for the ground-based sensors. The HP 735 serves as the primary processor and data manager, and handles the data base. Three PCs operate the radar, collect National Weather Service (NWS) weather maps, and operate the microwave radiometer. As many as two balloon systems operate from the trailer to obtain comparison data. During the test in the Los Angeles basin 27 August through 23 September 1993, a Marwin and CLASS were simultaneously operated. A TD MDS demonstration was held at White Sands Missile Range (WSMR) in early October 1993, and a final Project Manager, Electronic Warfare/Reconnaissance Surveillance and Target Acquisition (PM-EW/RSTA) technical demonstration is planned for September 1994.

*Private communication with E. Measure.

3. Combining Method

Cogan [3] briefly describes the merging algorithms, and lists several references where they are described in more detail. Figure 1 shows the basic concept of the method. The ground-based systems provide detailed soundings for the lower troposphere, and the satellite sounder covers the atmosphere from approximately 2 or 3 km to 30 km. Profiles from the ground-based systems are combined to form a single multivariable sounding. The satellite sounding is weighted relative to the ground-based sounding location and time, and they are merged. Normally, satellite and ground-based profiles overlap (except temperature when no microwave data are available). If the profiles do not overlap, the satellite data for each variable are extrapolated to the uppermost level of the ground-based profile. For each variable, routines within the merging program adjust the satellite profile starting at the satellite sounding level immediately above the highest level of the ground-based profile. The several merged profiles are entered into a file to form a combined sounding. Figure 2 shows a block diagram of the software that generates the combined sounding and computes layer values. The values are input into routines to generate meteorological (MET) messages.

The software package contains C functions that convert the combined sounding into two types of MET messages: the computer MET message (MET-CM) and the Tacfire version of the Air Weather Service (AWS) message. These messages are produced every 15 min and, in the September demonstration, will be sent as ASCII files to the Computer Assisted Artillery Meteorology (CAAM). Demonstration satellite sounding files (one per swath) will be sent to the CAAM as soon as they are received and processed. Cogan [7] gives an algorithm for converting a sounding to an artillery computer MET message. The AWS message is in standard World Meteorological Organization (WMO) format, requiring no computation of layer values.

Miers et al. [4] and Cogan [3] present accuracies for the same types of systems as those in the TD MPS, based on published values in a number of papers such as Strauch et al., [8] Lawrence et al., [9] and Weber and Weurtz. [10] This report presents samples of data gathered by the TD MPS and comparisons with rawinsonde values. Comparisons between two rawinsonde systems gives an idea of the accuracy of the rawinsonde data. [11]

COMBINED SOUNDING CONCEPT

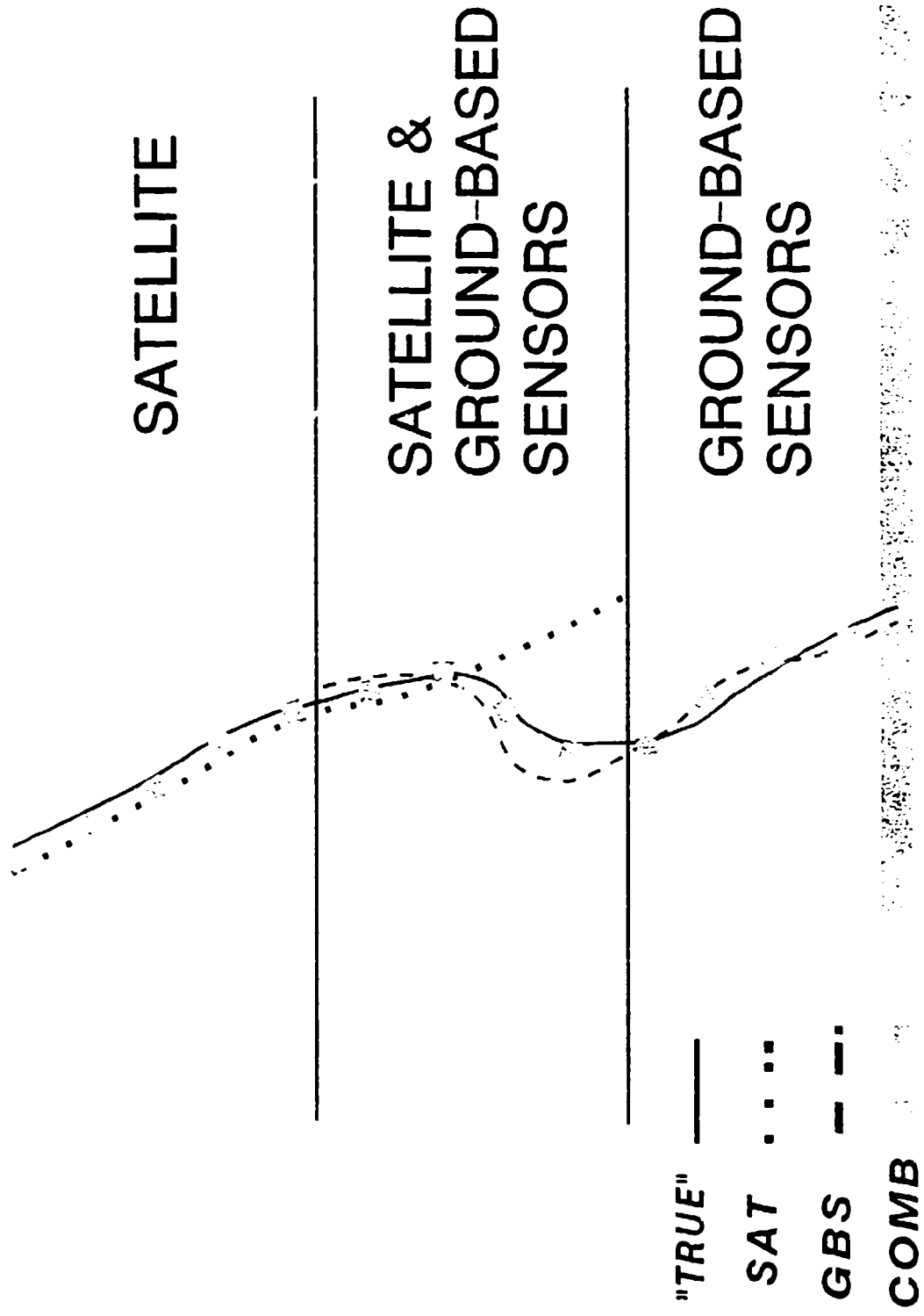
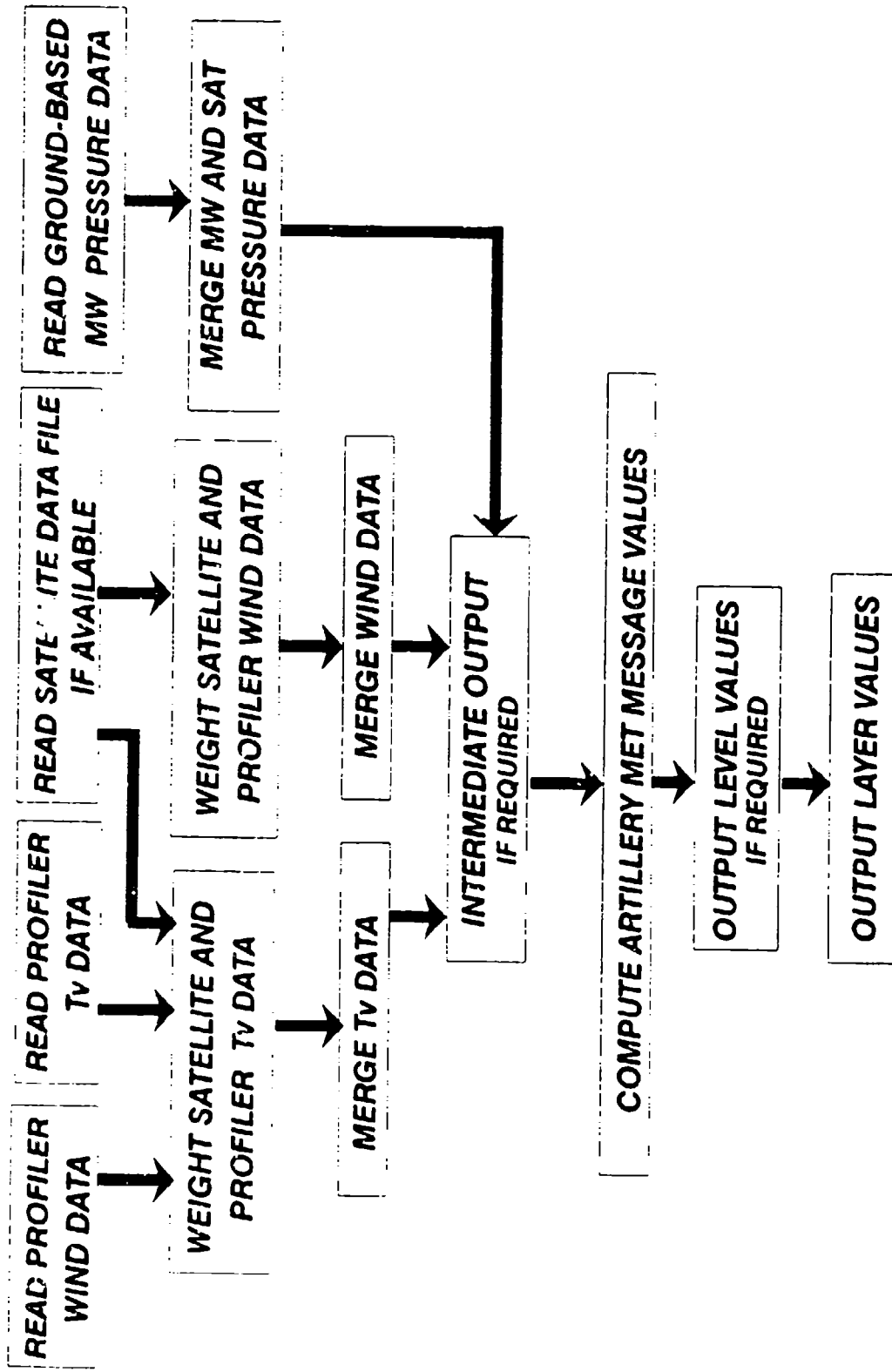
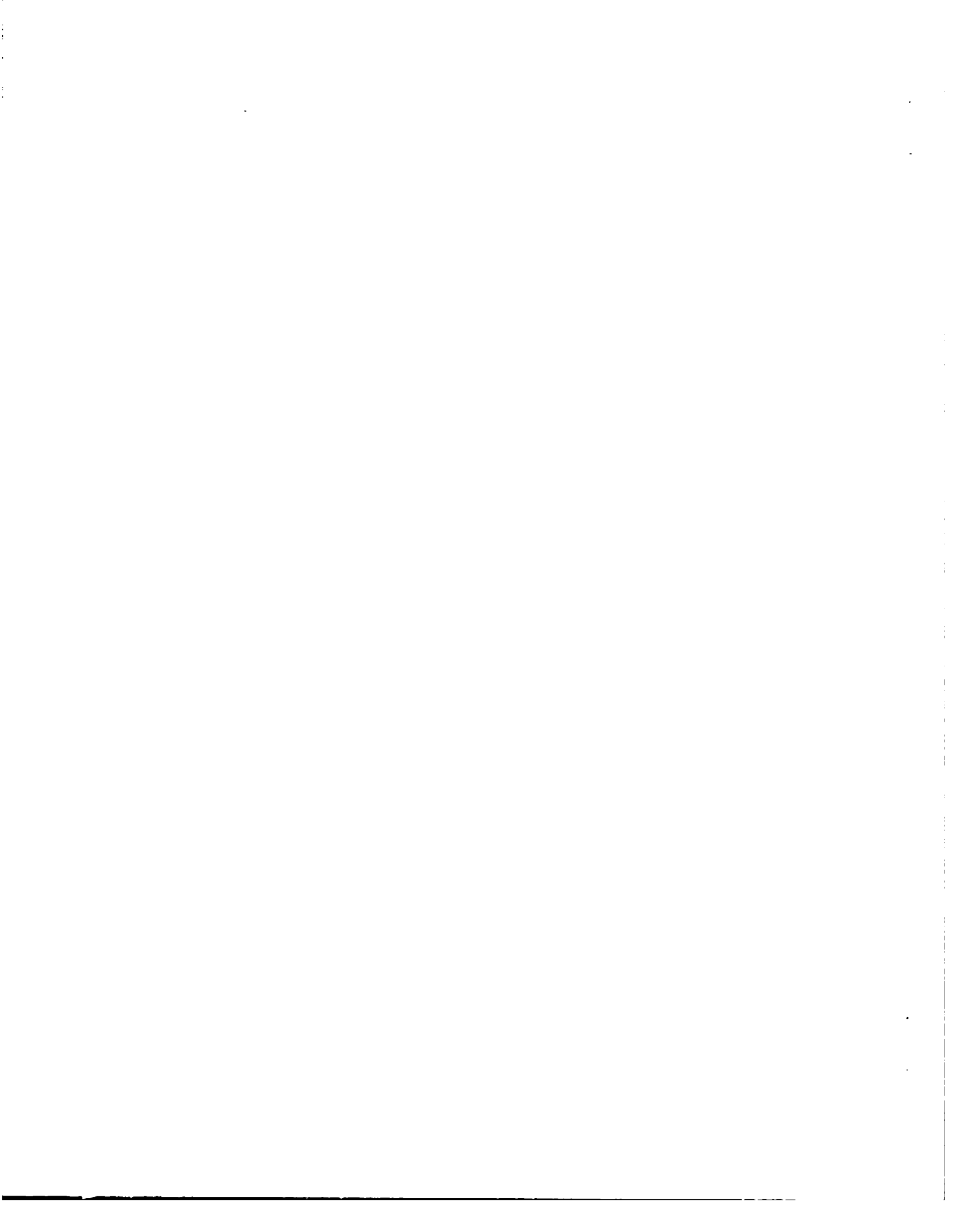


Figure 1. Combined sounding concept. Satellite and ground-based data are merged to form a more accurate sounding for the atmosphere from the surface to the highest satellite sounding level.



13 Figure 2. Block diagram of the combined sounding program and computation of layer values for input to MET messages.



4. Data

The combining software produces output in a variety of formats including MET-CM and AWS (Tacfire) messages. The system is capable of producing additional output in alpha-numeric text, graphical charts, and imagery. The examples in this section provide samples of output types.

Figure 3 shows a combined sounding in the format of a MET-CM message. The data are in standard artillery format (wind direction in units of tens of mils). The current satellite terminal software calculates geostrophic wind only as high as the 100 mb level, and temperature output reaches as the high as 10 mb level. Future versions of the software will calculate wind velocity as high as 10 mb.

```
MET;CM;Q:1;POSI:323064;DTI:03/20.7/0;HGT:128;ATMS:872;  
00/282/006/311.4/0872,01/205/007/308.0/0862,02/205/008/303.8/0839;  
03/196/006/300.3/0801,04/099/006/296.0/0757,05/585/002/291.6/0714;  
06/024/009/287.3/0673,07/020/016/282.9/0634,08/032/015/278.6/0596;  
09/013/017/274.2/0561,10/627/019/269.9/0526,11/609/023/265.8/0494  
12/604/026/260.4/0448,13/609/030/253.5/0392,14/621/035/247.1/0342;  
15/630/040/240.8/0297,16/637/045/234.2/0257,17/003/051/227.3/0222;  
18/009/057/220.8/0190,19/016/061/215.0/0163,20/023/065/210.8/0138;  
21/030/067/208.3/0118,22/ / /206.1/0100,23/ / /206.6/0084;  
24/ / /207.5/0071,25/ / /208.8/0061,26/ / / /
```

Figure 3. Tabular output from the combining software on the TD MPS in the format of the MET-CM artillery MET message.

In figure 3, wind values appear up to line 21, and temperature values appear up to line 25. A blank field indicates missing data.

Figure 4 presents a chart of radar profiler wind velocities in the form of standard wind arrows. Speeds are in meters per second instead of knots (a full barb indicates 10 m/s). Soundings were made every 15 min and displayed on the chart every half hour. The abscissa is time in hours (UT), from 1200, 8 September (right) to 0330, 9 September 1993 (left). The color scale gives an indication of wind speed. The data were taken during an experiment in the Los Angeles basin in September 1993.

Figure 4 also shows several interesting MET phenomena. The marine boundary layer decreased in thickness from approximately 2 km at the beginning of the period to approximately 800 m at approximately 2100 (1400 PDT), 8 September 1993. Above the boundary layer, an easterly flow became light and variable for a few hours near 2300 (1600 PDT), 8 September 1993, turning westerly to a height of approximately 1.5 km. Apparently, the marine boundary layer thickened later in the day. The profiler shows the complexity of the flow within the boundary layer and a few kilometers above it.

Figure 5 shows an image of RASS temperatures averaged and displayed each half hour from 1200, 7 September to 0000, 8 September 1993. The scale below the abscissa indicates temperature in celsius. The half-hour temperatures (100-m layers) displayed in the column centered at 1300 show cool air (approximately 24 to 25 °C) in the lowest 450 m, capped by a zone of warmer air (approximately 26 °C) between 450 and 650 m, with a lapse rate of approximately 8 °C/km (approximately 18 °C at 1600 m). The early morning inversion persisted until approximately 1700 to 1800 (1000 to 1100 PDT) with significant heating of the lower part of the boundary layer occurring afterwards. Although some of the temperatures at the far upper left of the image may be spurious (left column above 1 km and next column to right above 1.2 km), it appears that an inversion begins to form at approximately 1 km starting between 2100 and 2200 (1400 and 1500 PDT).

Figure 6 displays combined soundings of wind velocity over a 10-hr period, from 1600, 11 September to 0200, 12 September 1993. Radar wind profiles appear every 30 min; however, satellite wind profiles generally are available every 2 to 6 hr. The adjustment to the satellite winds are only slight because of the light, variable wind at uppermost radar heights (below 5 km). Slight changes in wind speed at the lowest three satellite levels show up as minor color variations. A temporary shutdown of the radar produced the gap in data at 2230.

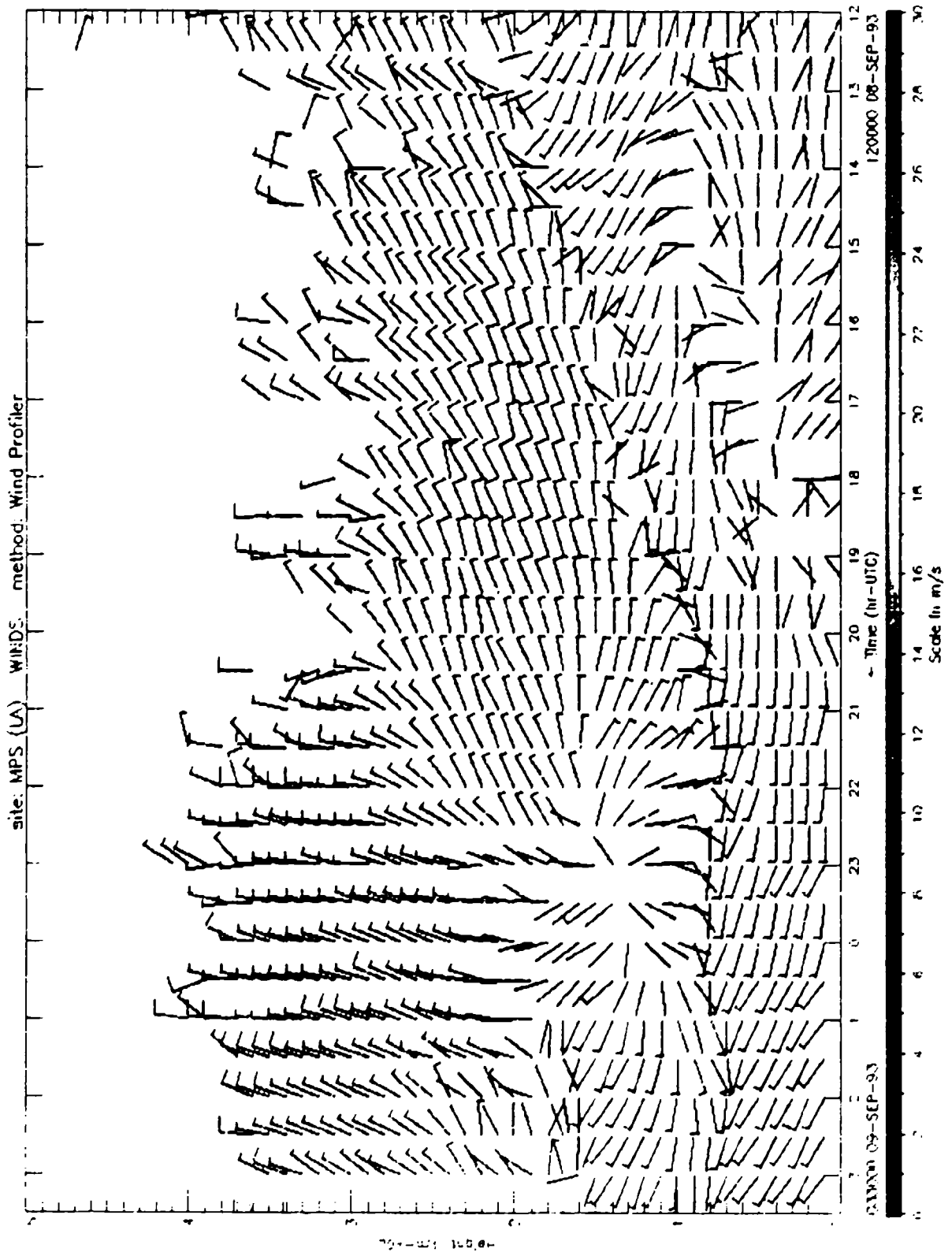


Figure 4. Time-height display of wind velocity profiles from the 924 MHz radar profiler. Wind arrows of full and half barb represent 10 and 5 m/s, respectively. The site is Claremont, CA (Los Angeles basin). Soundings derived using 15 min of data, and displayed every half hour.

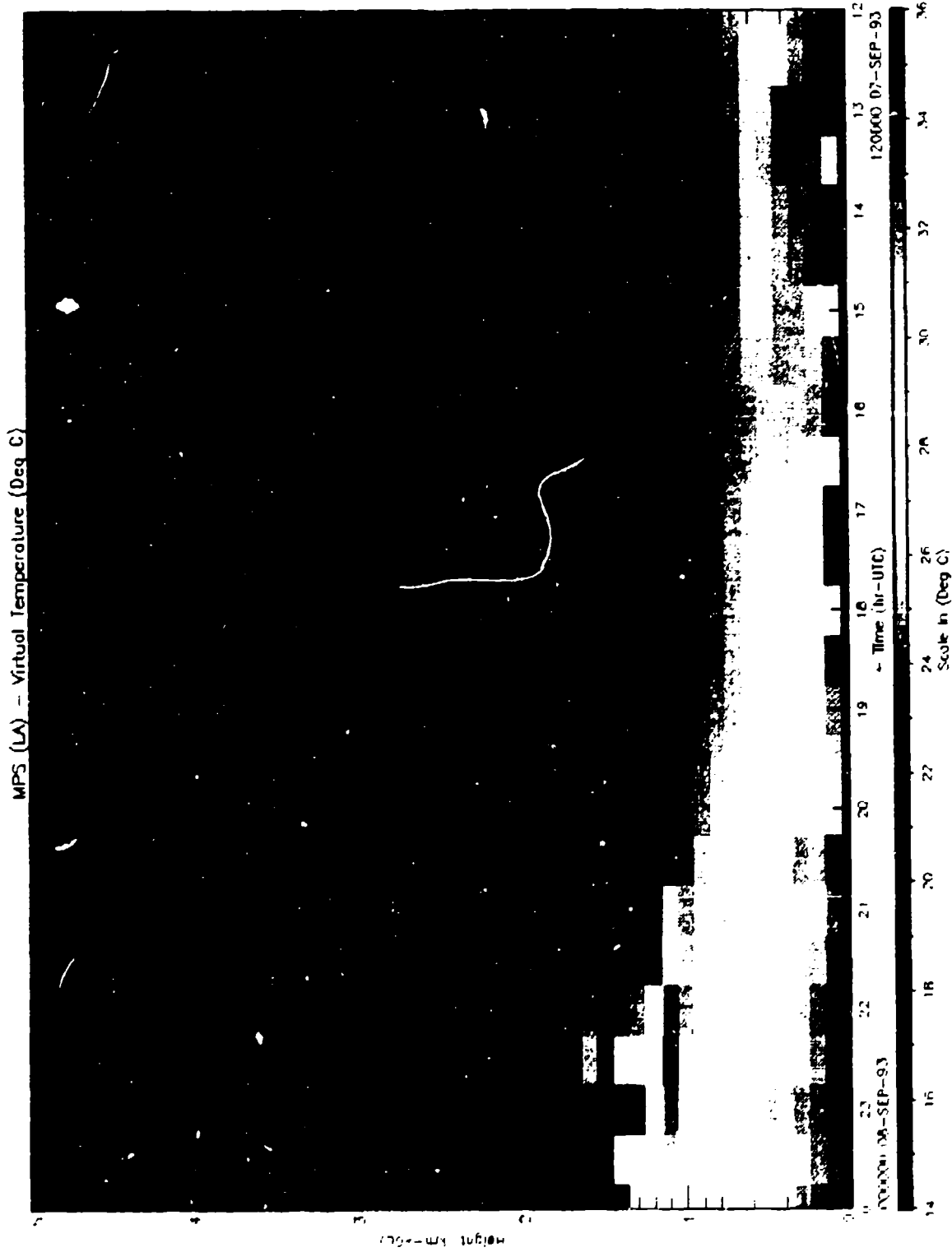


Figure 5. Time-height display of virtual temperature from the RASS. Missing data adjacent to the surface were removed by the quality control routine.

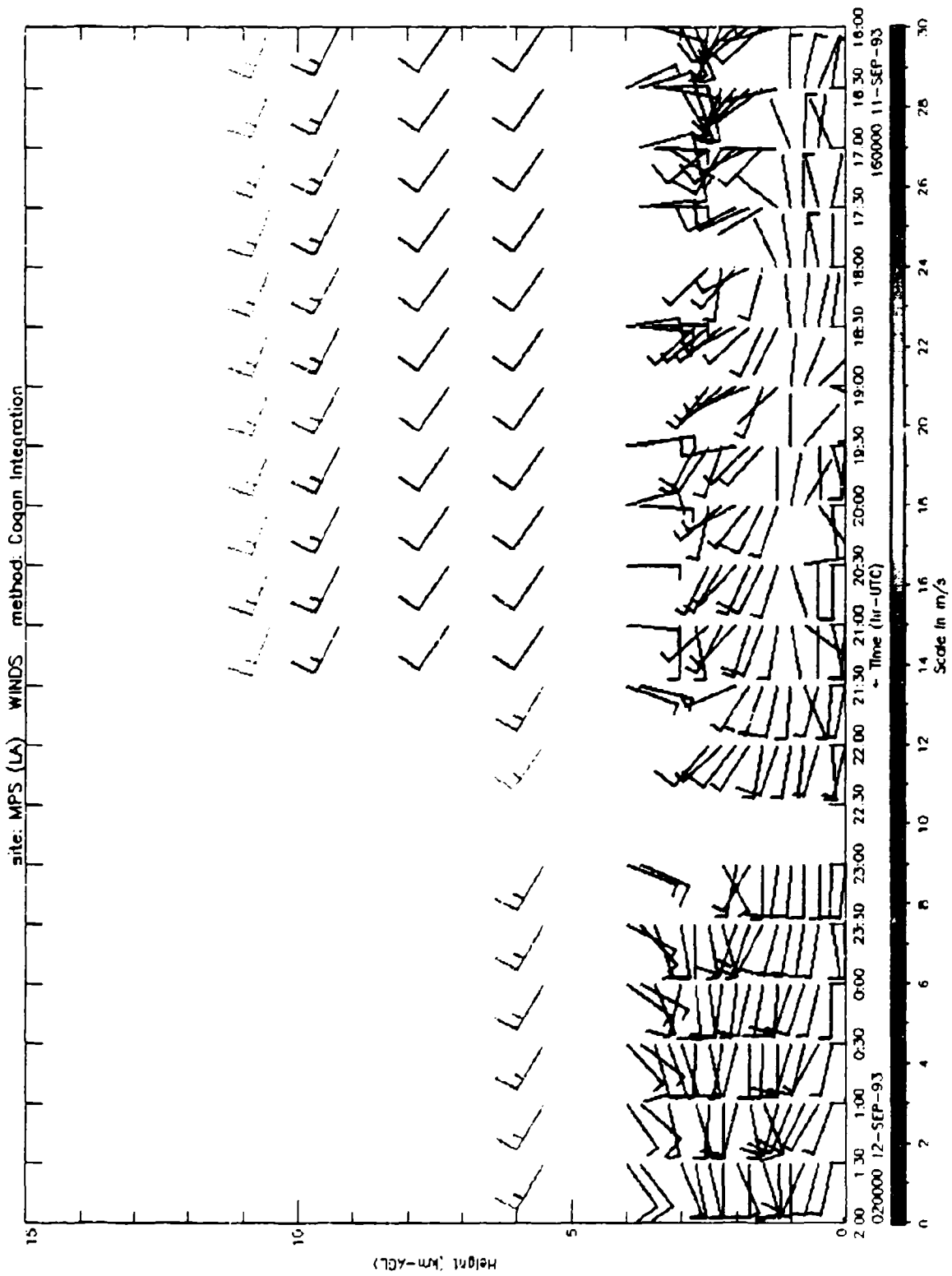


Figure 6. Time-height display of combined wind velocity profiles derived from radar profiler and satellite data.

5. Comparisons

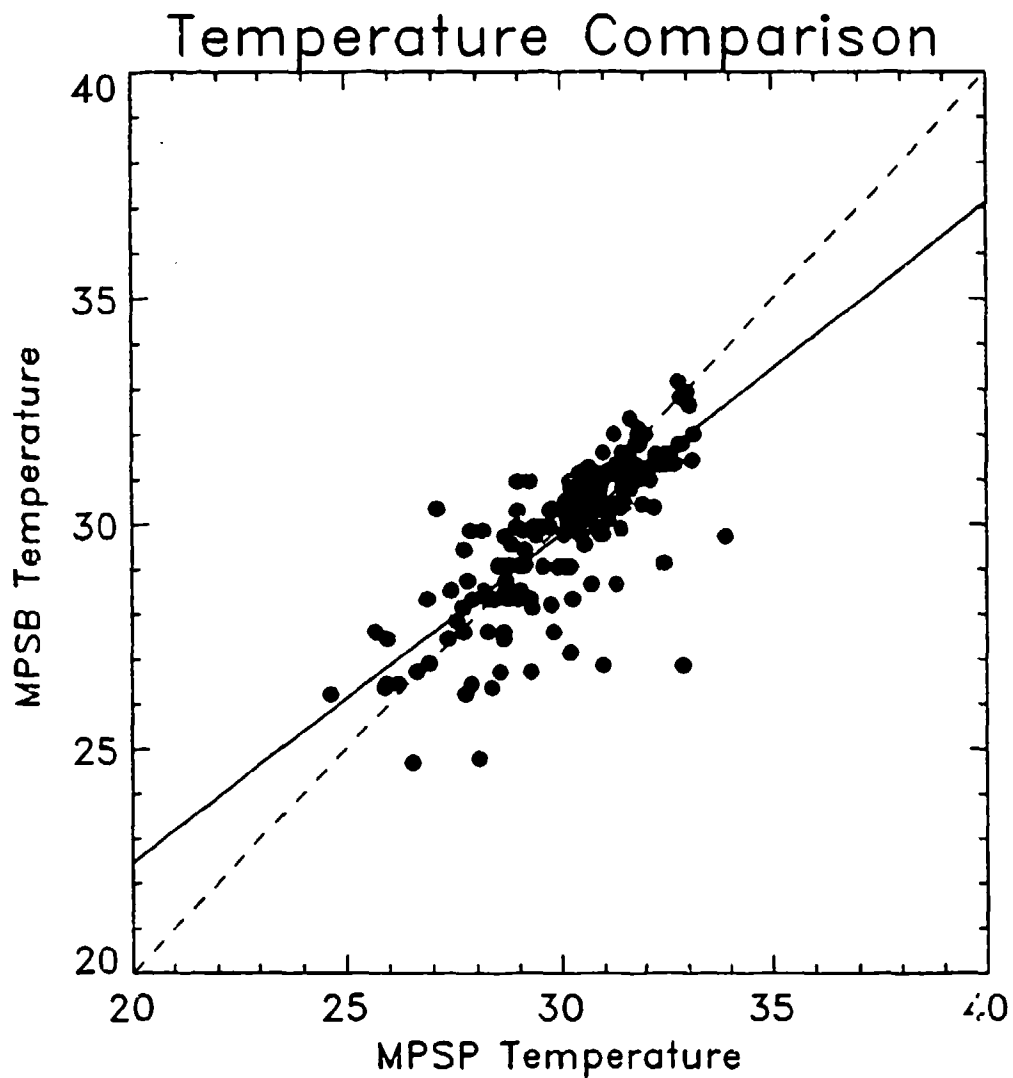
RASS, satellite, and combined RASS and satellite virtual temperature profiles were compared with rawinsonde soundings. Figures 7 through 9 show virtual temperature from each of the systems, plotted against rawinsonde data. Figure 7 presents the comparison for RASS. Mobile Profiler System Balloon (MPSB) indicates the rawinsonde (balloon) data. Time is given in hours, minutes, and seconds as a 6-digit number. Figure 8 presents the same type of information for satellite data. The standard deviation of the differences for the satellite profile exceeds the standard deviation of RASS by slightly less than a factor of two. The mean difference also is approximately two but in the opposite direction. Figure 9 shows the comparison for the entire combined sounding. The standard deviation drops to a value lower than the value for the satellite data, and the mean difference falls to a magnitude lower than the satellite or RASS data. The standard deviation and mean difference for the combined sounding are on the good side of average (approximately 1.5 to 2 K and approximately 0.5 K, respectively).

Figure 10 presents the same type of comparison for radar profiler wind speeds. The standard deviation is in line with values reported in the literature. [4] The mean difference is small (-0.13 m/s). No attempt was made to compare satellite or merged wind speeds because of highly variable errors in the satellite soundings.

Based on values in the literature, [4] standard deviations for satellite geostrophic winds of approximately 5 to more than 15 m/s were expected, depending on the atmospheric situation. A potential source of disagreement between the satellite and rawinsonde could arise when the satellite sounding is far from the balloon location, especially if the launch site is under a ridge or trough.

To maximize the possibility of a merged sounding, the algorithm was set to accept the nearest satellite sounding as distant as 320 km. Also, the site was under an upper ridge for the period these data were gathered. Under these conditions, large differences could occur between the rawinsonde and satellite wind speeds. The use of satellite soundings as much as 6 hr distant

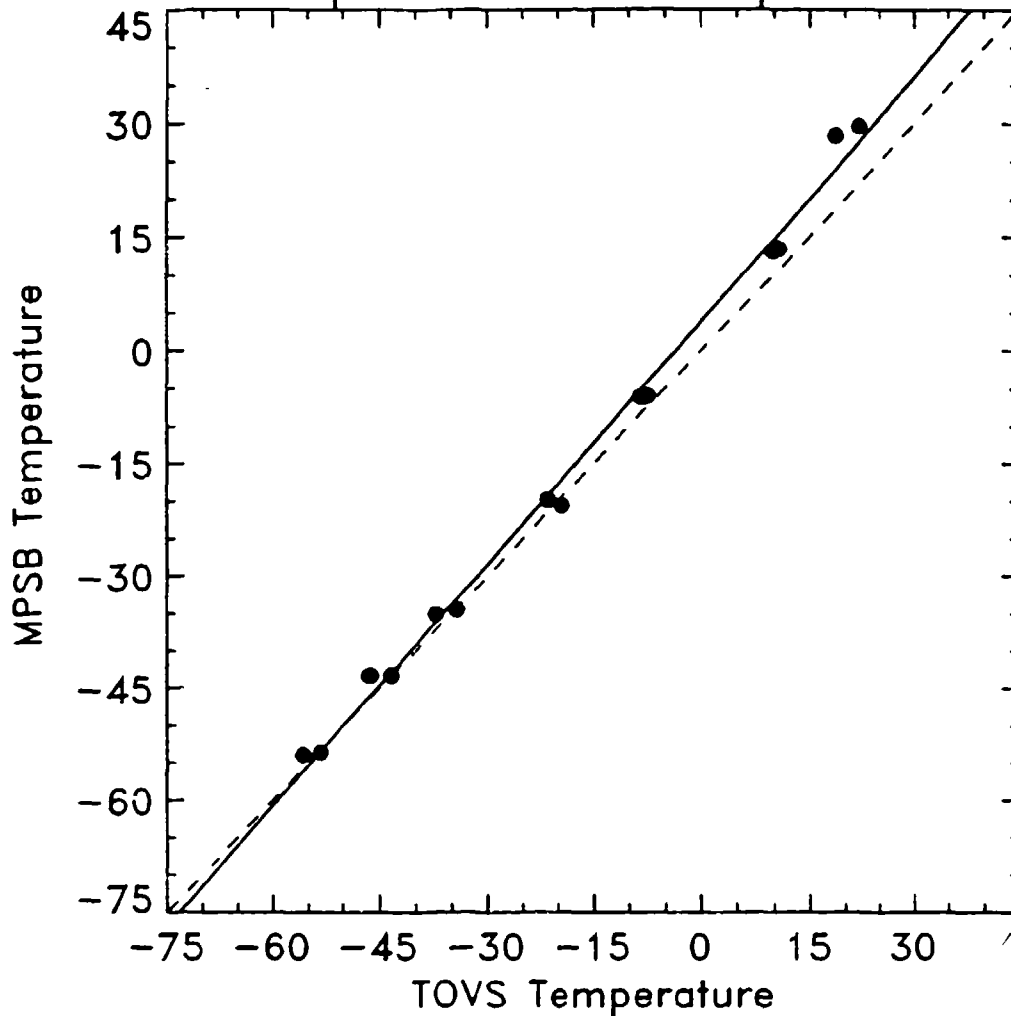
from the rawinsonde, to augment the possibility of a merged sounding, could have contributed to the large differences observed in wind speed. Later comparisons, between satellite and rawinsonde wind speeds in a more zonal flow, suggest that distances in time or space may be part of the cause of the large differences noted.



130000, 10 September 1993 to 190000, 10 September 1993
 Los Angeles - Claremont
 Number of Points = 215
 Height Range (km-AGL): 0.10 - 1.60
 LSF: Slope = 0.73 Intercept = 7.79
 Standard Deviation of Differences: 1.06
 Mean Difference: -0.29

Figure 7. Virtual temperature (°C) comparison between RASS and rawinsonde. MPSB indicates rawinsonde.

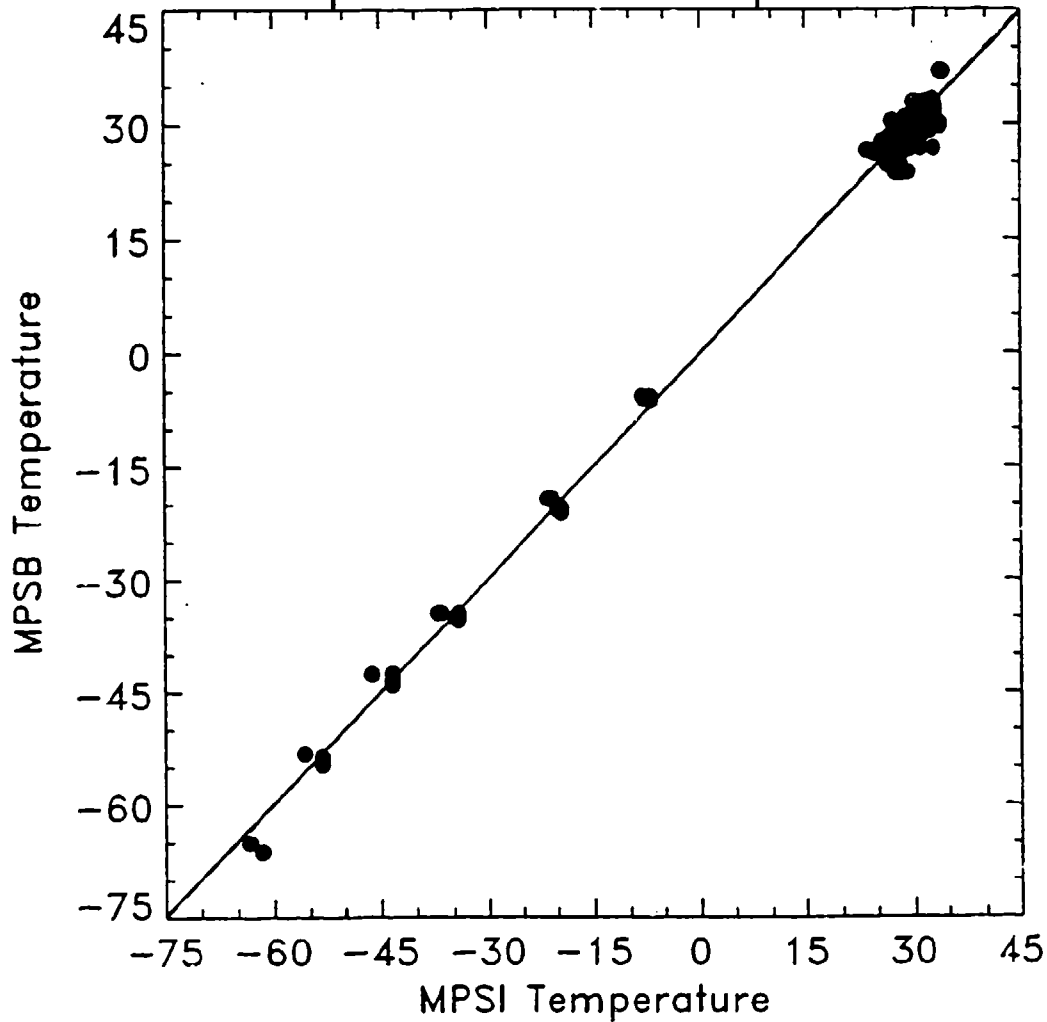
Temperature Comparison



130000, 10 September 1993 to 190000, 10 September 1993
Los Angeles - Claremont
Number of Points = 14
Height Range (km-AGL): 1.10 - 12.00
LSF: Slope = 1.08 Intercept = 3.85
Standard Deviation of Differences: 2.97
Mean Difference: 2.41

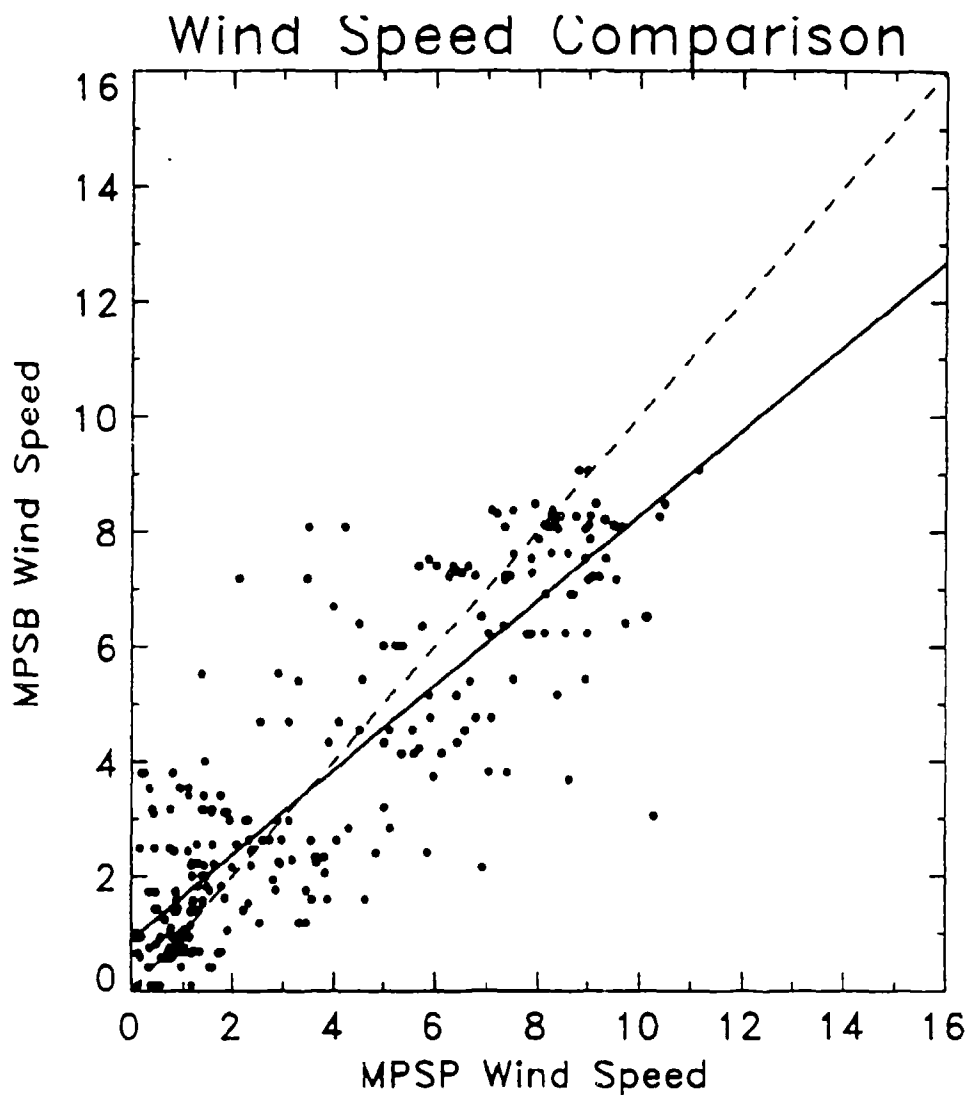
Figure 8. Virtual temperature (°C) comparison between satellite and rawinsonde.

Temperature Comparison



130000, 10 September 1993 to 190000, 10 September 1993
Los Angeles - Claremont
Number of Points = 334
Height Range (km-AGL): 0.00 - 13.80
LSF: Slope = 0.99 Intercept = -0.11
Standard Deviation of Differences: 1.48
Mean Difference: -0.16

Figure 9. Virtual temperature (°C) comparison between the combined sounding and rawinsonde.



140000, 08 September 1993 to 190000, 08 September 1993
 Los Angeles, CA
 Number of Points = 269
 Height Range (km-AGL): 0.10 - 3.50
 LSF: Slope = 0.74 Intercept = 0.90
 Standard Deviation of Differences: 1.61
 Mean Difference: -0.13

Figure 10. Wind speed comparison (m/s) between the radar profiler and rawinsonde.

In one case (not shown) 8 September 1993, the ground-based sounding occurred near the midpoint between two satellite passes, approximately 6 hr apart (earlier passes closer by 3 min). The wind speeds from the earlier pass deviated from those measured by the rawinsonde by 2 to 4 m/s, but the later one had differences of 12 to 16 m/s. The altitude ranged from approximately 5 to 10 km, and the two satellite soundings occurred within 100 km of the test site. This high variability in wind speed is in line with results reported by Miers et al. [4]

The mean and standard deviation vary with the time window of the comparison. The time window is defined as the period for which sensor data are compared with comparison standard data. A window of 15 min for the RASS and rawinsonde comparison means virtual temperatures from RASS taken during the ± 15 min surrounding the launch time of a rawinsonde are compared with virtual temperatures from the rawinsonde. The window does not symmetrically surround each rawinsonde data point because a rawinsonde sounding is not instantaneous. A typical rawinsonde balloon rises at approximately 305 m/min (1000 ft/min), reaching the uppermost level of the RASS (approximately 1.6 km) in slightly less than 5 min. For time windows of 15 min or more, the increasing time offset with height normally is not significant for RASS heights.

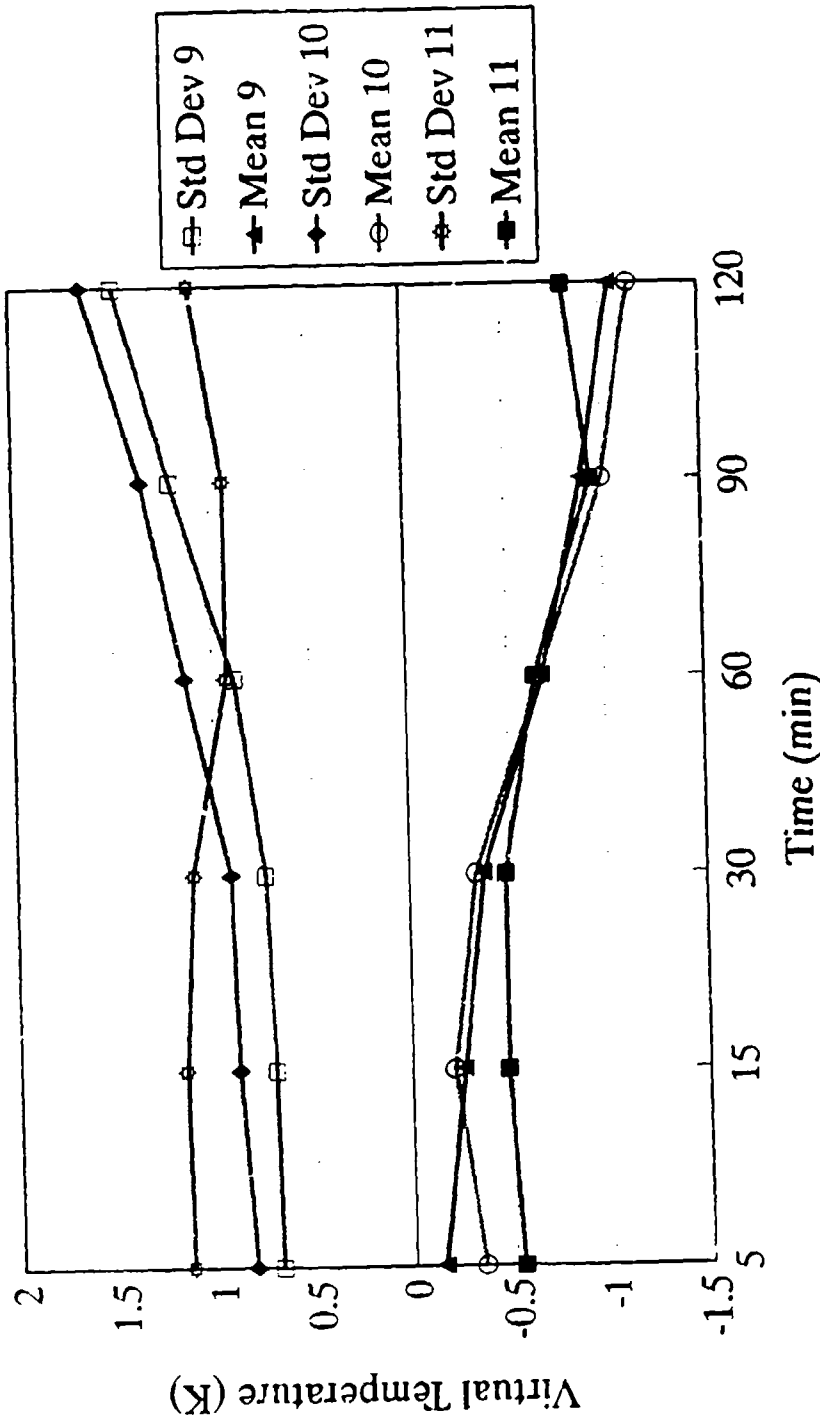
For comparisons with satellite or combined soundings, the use of the rawinsonde launch time may seriously affect the results under changing atmospheric conditions. Use of the midpoint time of the rawinsonde sounding, or a finer division such as a time for every kilometer may be more accurate; however, at the time this report was prepared the software used rawinsonde launch times.

RASS and combined sounding virtual temperatures were compared with values from four rawinsonde soundings covering approximately 5 hr on each of three days (9 through 11 September 1993). Each rawinsonde sounding consisted of two sets of data, one from a Marwin and one from a CLASS system, taking measurements from the same sonde. Figure 11 shows RASS comparisons for several time windows from 5 to 120 min for the three 5-hr periods. The curves for the mean values (bottom set of lines) roughly follow one another. The mean differences relative to the rawinsonde values are -0.5 K or less for 30-min windows. For increasingly larger time windows, the differences became more negative, approximately -1 K for 90- and 120-min windows. A trend to larger magnitudes also occurred for two of the standard deviation curves, from approximately

0.7 to 0.9 K for windows as large as 30 min to approximately 1.5 or 1.6 K for windows of 120 min. However, the standard deviation curve for 11 September 1993 behaved differently. The values began at approximately 1.1 to 1.2 K for windows of 5 through 30 min and decreased to approximately 0.9 K for windows of 60 and 90 min, and increased again to approximately 1.1 K for windows of 120 min.

RASS Comparison

9-11 Sep 1993 - Claremont, CA



Layer: 0.2 km, Time interval: 15 min, Height range 0 - 1 km.

Figure 11. Virtual temperature ($^{\circ}\text{C}$) comparison between RASS and rawinsonde showing mean and standard deviations on each of three days. The time window varied from 5 to 120 min.

Figure 12 presents similar types of curves for combined soundings, except the windows are 30 through 180 min. The mean values (lower curves) show a trend to increasingly negative values as the time window increased. The standard deviations increase with time window size, although, the line for 11 September 1993 decreased by 0.04 K from 30 to 60 min followed by a slight increase to the same value (1.5 K) at 180 min. Most noticeable are the much larger standard deviations for 9 September 1993, which appear to be a result of the satellite sounding (adjusted) having a large mean difference of approximately 2.7 to 2.9 K and a standard deviation of approximately 2.3 to 2.4 K. The merging and adjustment process also eliminates the satellite temperatures below approximately 3 K, thereby reducing the mean difference and standard deviation of the satellite data.

Adjusted data refer to satellite profiles that were established in the merging algorithm using the uppermost level of the ground-based data. The magnitude of the mean differences (mmd) for the satellite soundings on the other two days were < 1 K and the standard deviations were a few tenths of a kelvin lower. As with any single station merging method, poor or unrepresentative input can be expected to lead to output with lower accuracies. During most of the Los Angeles experiment, the site was under a strong ridge, and the algorithm was set to accept satellite soundings as distant as 320 km. It is possible that one or more satellite soundings on 9 September 1993 were too far from the site considering the atmospheric situation.

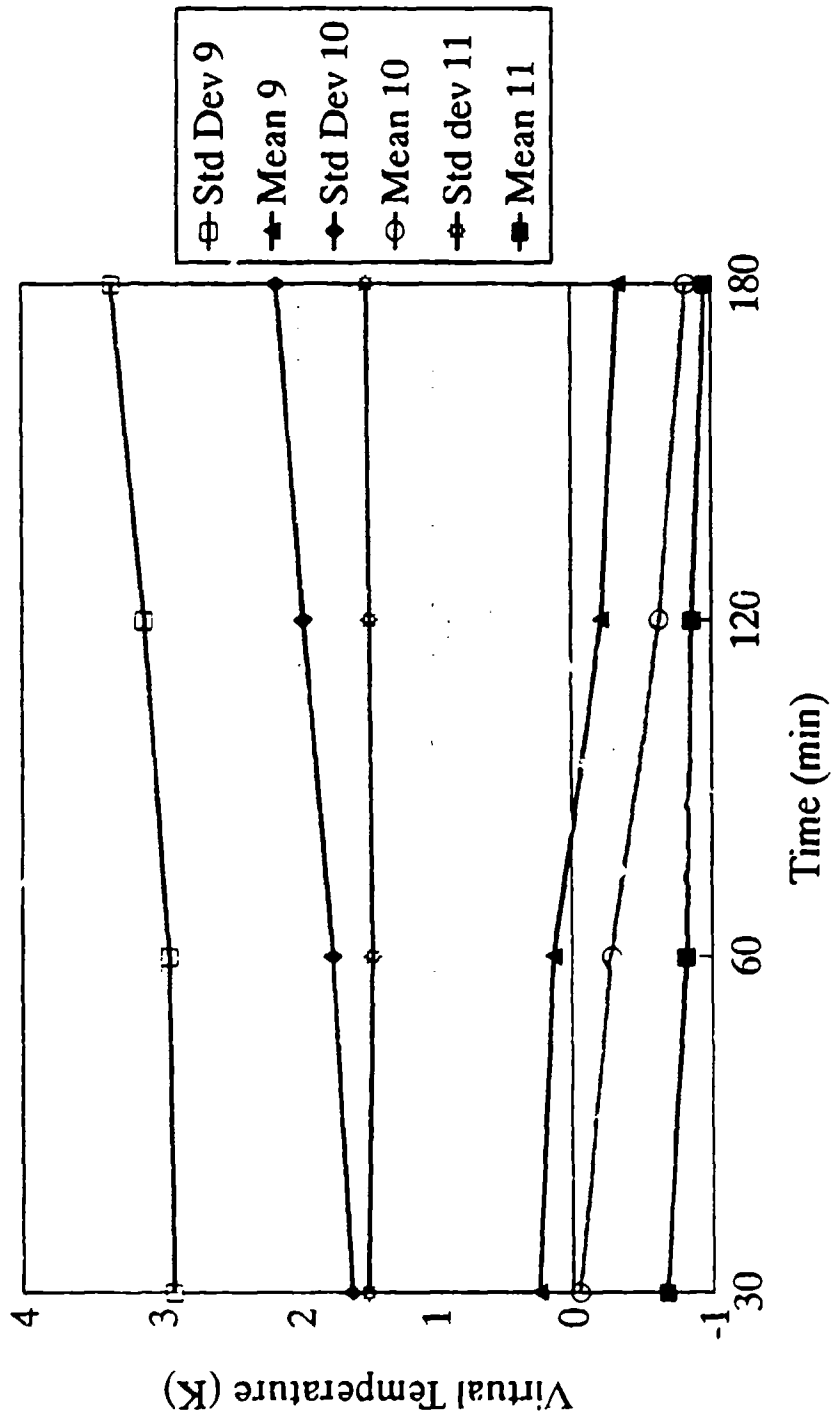
The ground-based microwave radiometer provided temperature data during the latter part of the Los Angeles experiment. Temperature profiles from the radiometer were compared with profiles from rawinsonde data (Marwin). Figure 13 shows a typical comparison made near 1800 (UT) on 14 September 1993. The points shown for the radiometer represent mean values for volumes of atmosphere, as opposed to point values from the rawinsonde. Therefore, an exact match of the profiles should not be expected, especially where inversions are present. Near the surface, the thickness of each volume is approximately 30 m, increasing to more than 2 km above 5 or 6 km. As seen in figure 13, the radiometer can follow inversions reasonably well near the surface but not above approximately 1 or 2 km. The radiometer temperatures were as much as 3 or 4 K higher than the rawinsonde temperatures (except very close to the surface), followed by several kilometers of lower values, and usually one higher value at the top. This last value represented a volume thickness extending

to the top of the atmosphere. The pattern held true throughout the period of 11 through 16 September 1993.

Wind soundings were presented side by side from two similar systems (Marwin and CLASS), receiving data from one sonde to determine the quality of the rawinsonde data. Figures 14 and 15 show examples of good and bad comparisons, respectively. The soundings are offset from one another on the graphs for clarity. Poor matches are not frequent. In figure 14 the wind speeds and directions closely follow one another, generally within 1 m/s and 10°.

Combined Sounding Comparison

9-11 Sep 1993 - Claremont, CA



Layer: 0.2 km, Time interval: 15 min, Height range: 0 - 15 km.

Figure 12. Virtual temperature ($^{\circ}\text{C}$) comparison between combined soundings (RASS and satellite) and rawinsonde showing mean and standard deviations on each of three days. The time window varied from 30 to 180 min.

Los Angeles, California (Claremont)

Balloon Launch: 9/14/93 11:05:00 LST
Radiometer: 9/14/93 11:05:58 LST

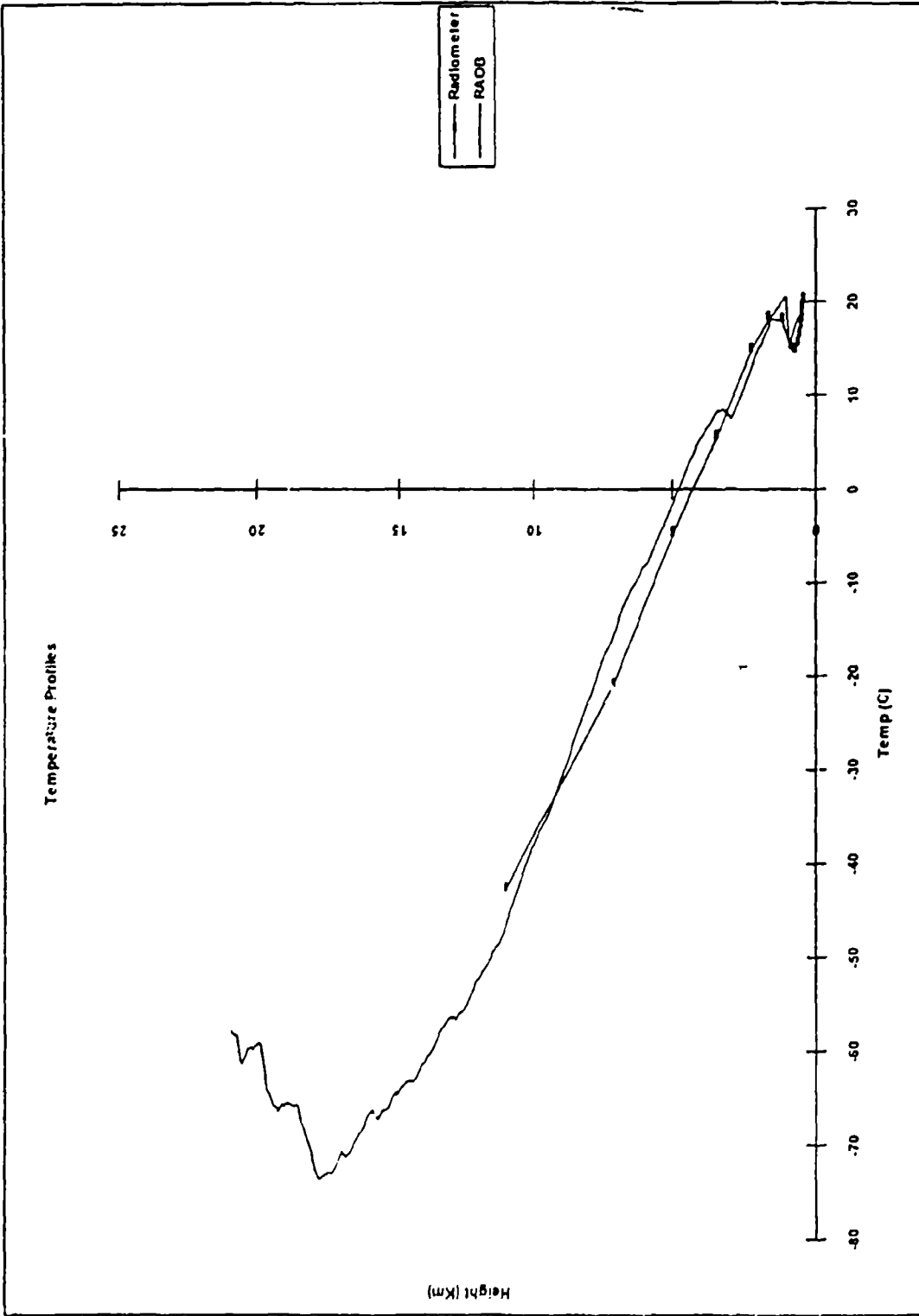


Figure 13. Temperature comparison ($^{\circ}\text{C}$) between the ground-based microwave radiometer and rawinsonde. The points shown for the radiometer represent mean values for volumes of atmosphere, as opposed to point values from the rawinsonde.

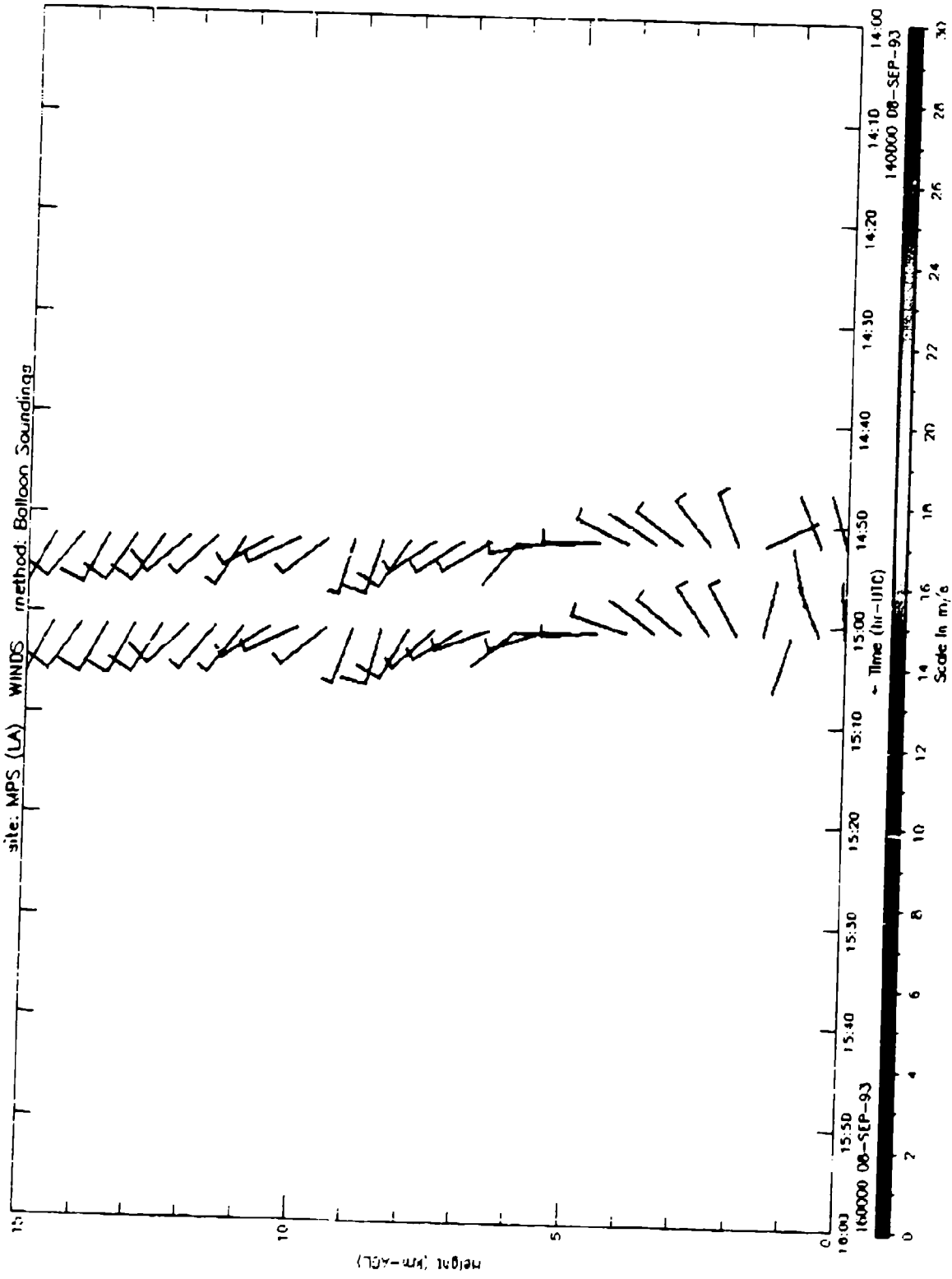
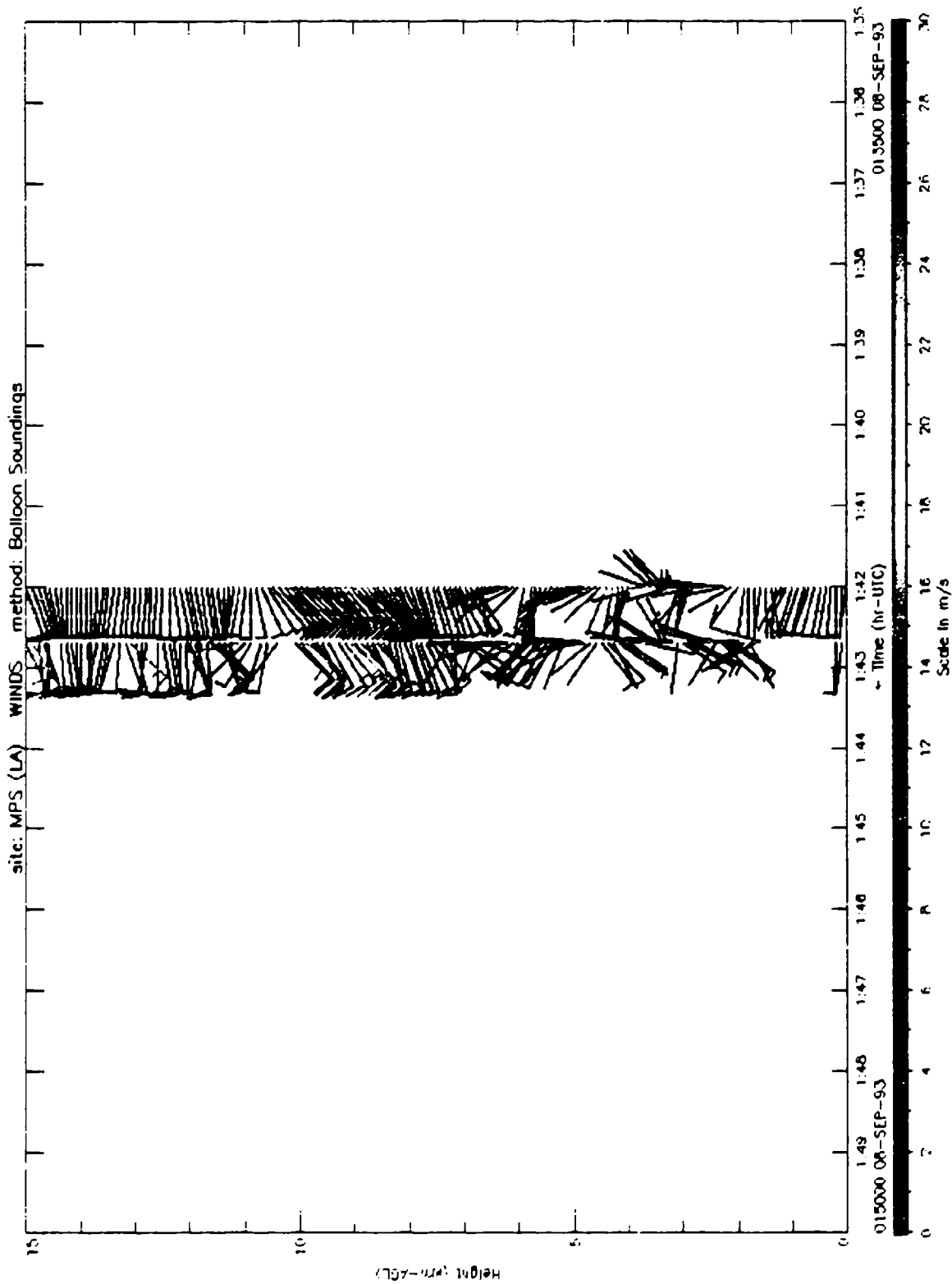


Figure 14. Wind velocity display comparing profiles from two rawinsonde systems, Marwin (right) and CLASS (left), using the same sonde. The profiles are offset from one another for clarity of presentation. (good case)



35 Figure 15. Wind velocity display as in figure 10. (poor case)

In figure 15, the wind speeds vary by ≥ 2 m/s at some levels, and wind direction varies considerably below 7 km and approximately 10 km. A possible partial explanation is that the Marwin software has more extensive built-in checks and somewhat smooths the data. When using a rawinsonde sounding as a standard, especially in light winds, be cautious. Determine that each sounding contains valid data, and apply appropriate quality controls.

6. Potential Problems and Solutions

A serious difficulty with the TD MPS is determining wind velocity profiles in regions of weak radar return. Normally, the radar provides good values of wind velocity up to the maximum height of useful return, 3 to 5 km in the current configuration. However, a detailed analysis of wind profile comparisons between radar and rawinsonde revealed a direct relation between strength of return and accuracy (relative to rawinsonde values).

Figure 16 presents a wind speed comparison in the same format as figure 10. In this example, the standard deviation of the differences and the mmd were larger than for figure 10. Comparisons for layers approximately 1-km thick indicate that the largest differences between wind speeds from radar profiler and rawinsonde were concentrated in the 1- to 2-km and 2- to 3-km layers, especially the latter. Figures 17a through 17d present the same type of analysis as figures 10 and 16, but for 1-km-thick layers (except the layer from 0.1 to 1 km). In figure 17a, the standard deviation and mmd are relatively low, partly caused by low wind speeds near the surface. For the next highest layer (figure 17b) the standard deviation and mmd more than double. Figure 17c shows a decrease in standard deviation and a very large increase in mmd for the 2- to 3-km layer. It appears that most of the error in figure 16 came from this layer. Figure 17d shows an increase in standard deviation, and the mmd dropped to 0.1 for the 3- to 4-km layer.

To understand why errors occurred in the middle layers (figures 17b and 17c), time height charts were generated for the period 1300 to 2000 UT, 11 September 1993. Figure 18 shows the four rawinsonde releases for this period. Each wind profile is a composite of the Marwin and CLASS profiles for that rawinsonde. The soundings may be compared with the radar wind profiles (half-hourly averages) for the same period (figure 19). A layer of weak or undetectable radar return lies between 2.5 and 3.5 km through much of the period, especially after 1600. A zone of weak signal often leads to unreliable wind velocities within the zone. Under light winds and in areas of significant wind shear, the differences between rawinsonde and radar wind measurements tend to be exaggerated. The differences in wind velocity may be attributed to the different types of measurements for rawinsonde and wind profiling radar, atmospheric variation during the comparison period (± 30 min from the rawinsonde launch time), and errors in the rawinsonde data. Variation in wind velocity over a short period

(figure 20) may be significant. Figure 20 shows wind profiles averaged and displayed every 5 min over a 1-1/2-hr period. Changes in wind direction over periods as short as 5 min were large above the marine boundary layer (approximately 800 m).

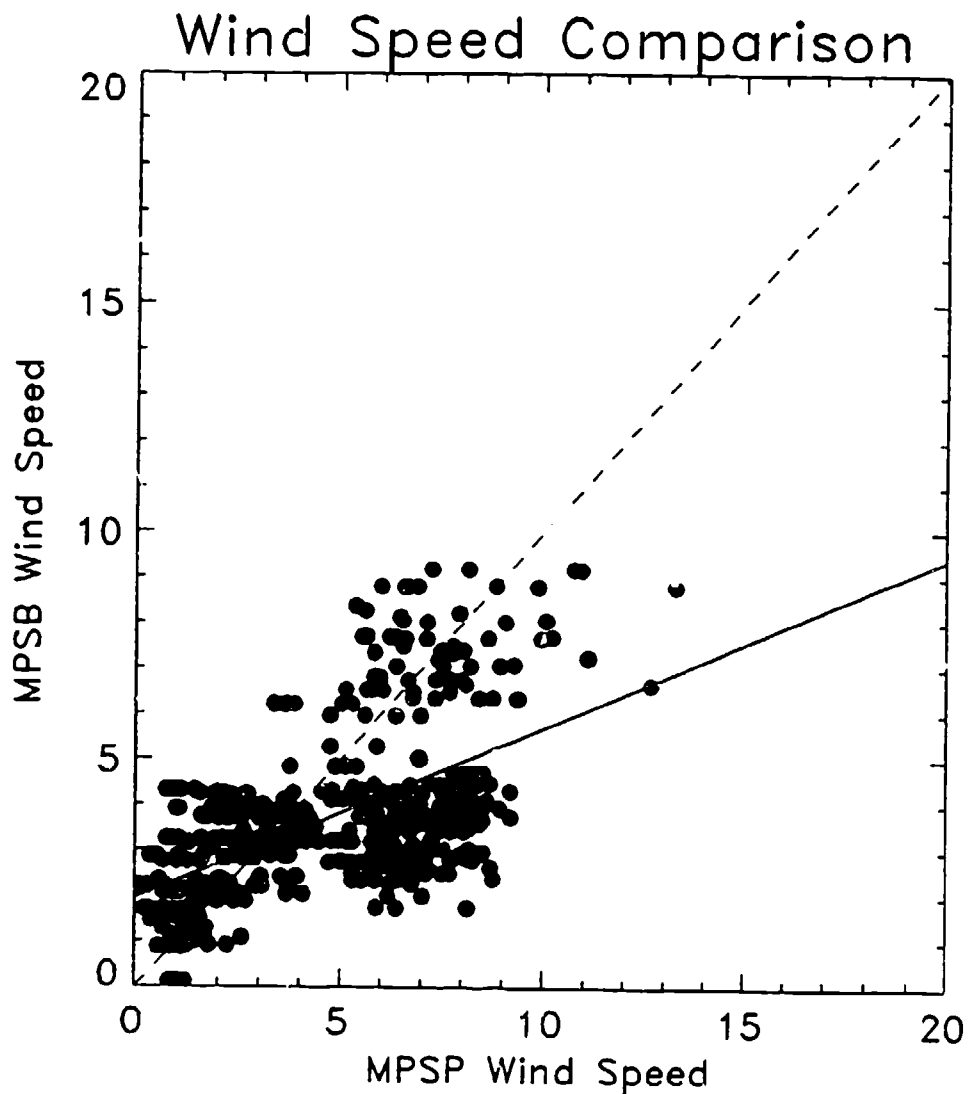
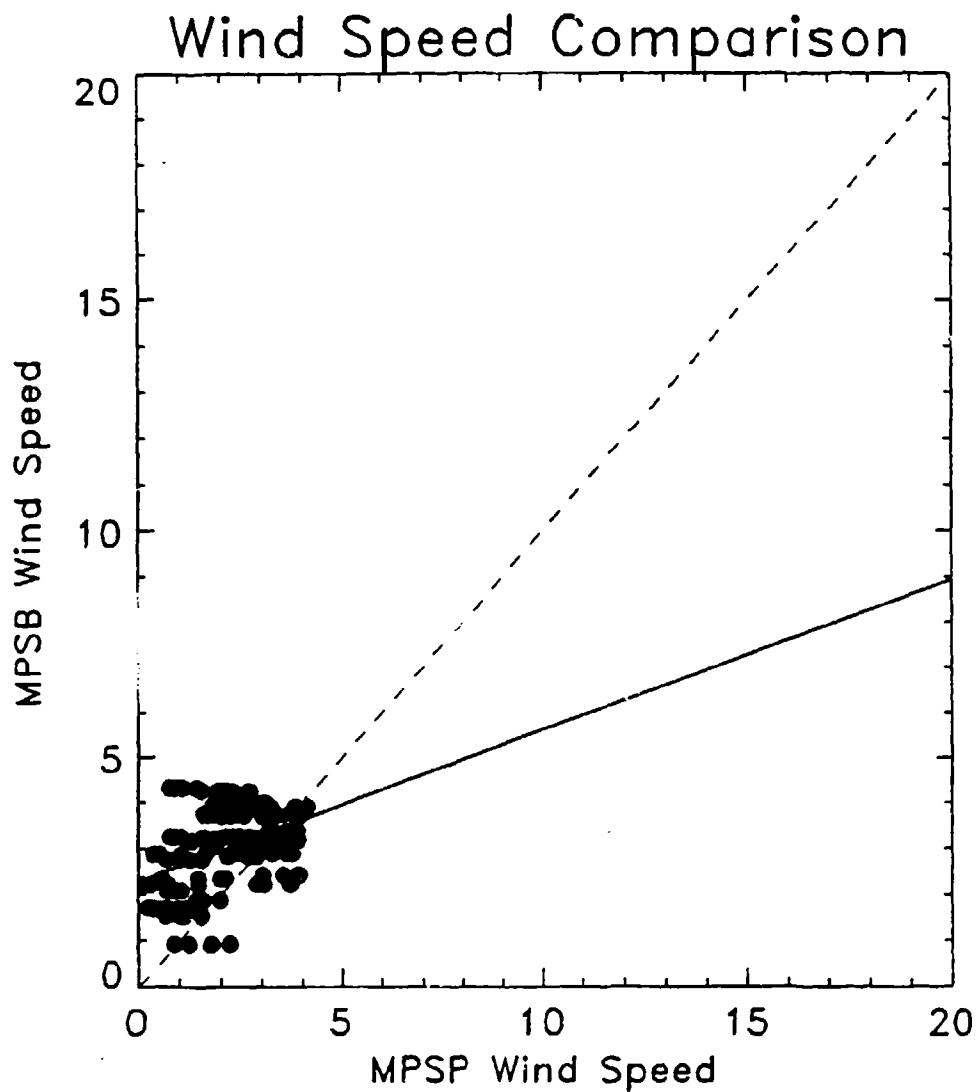
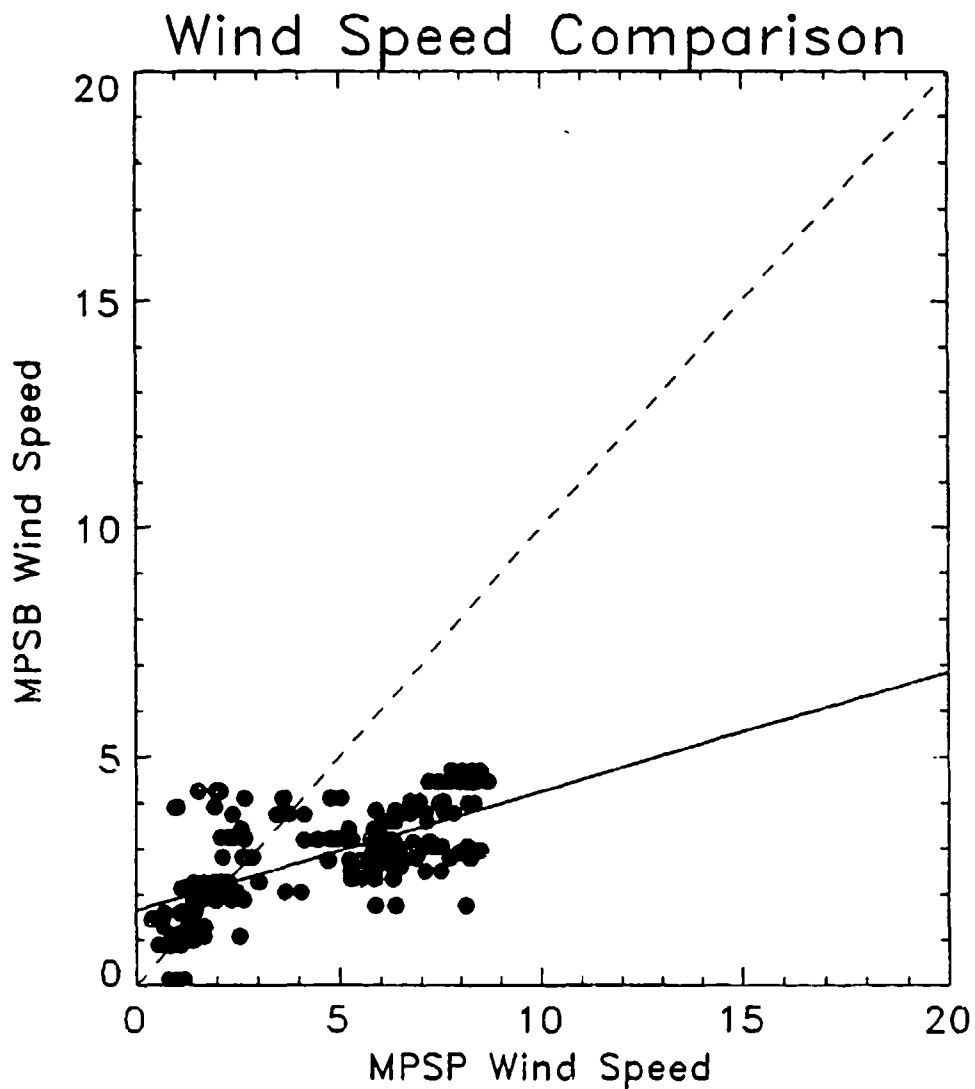


Figure 16. Wind speed comparison (m/s) between the radar profiler and rawinsonde for the period 1300-2000 UT, 11 September 1993.



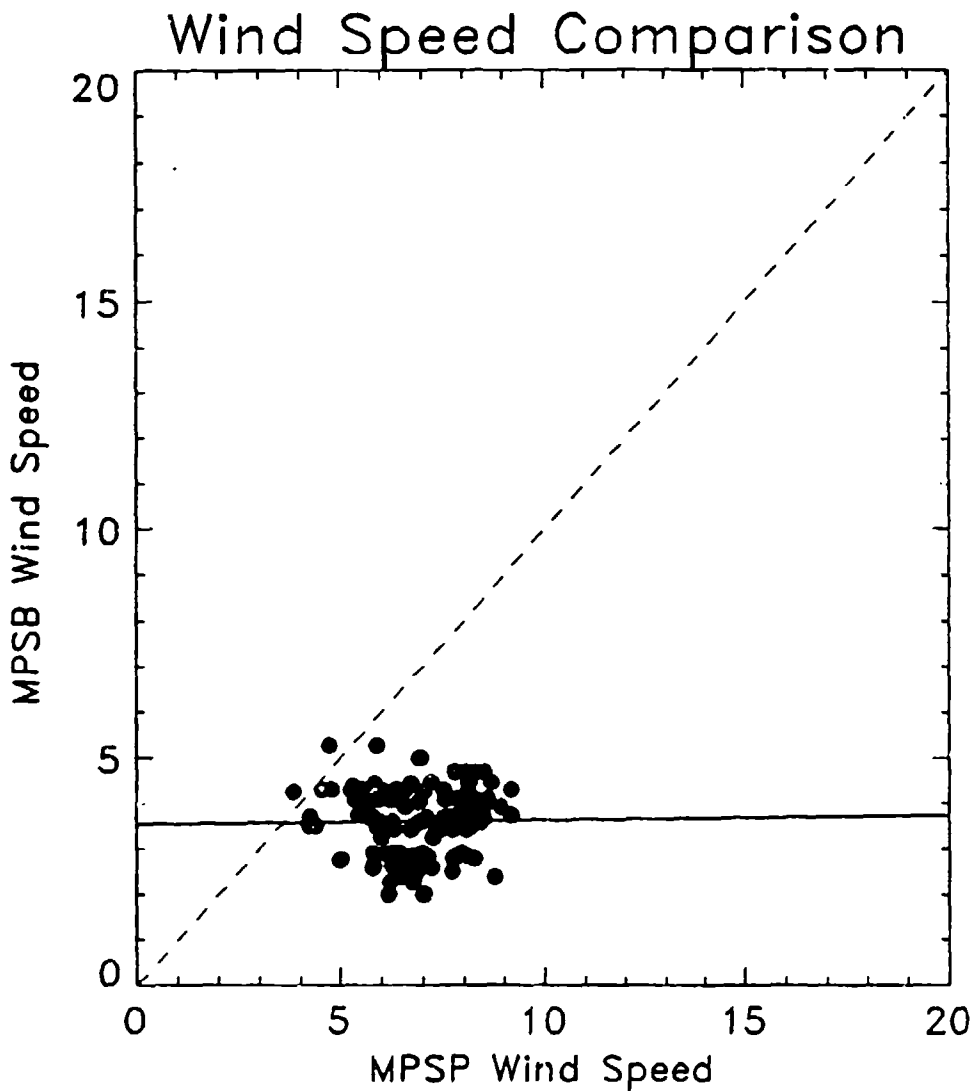
130000, 11 September 1993 to 200000, 11 September 1993
Los Angeles, CA
Number of Points = 170
Height Range (km-AGL): 0.10 - 1.00
LSF: Slope = 0.33 Intercept = 2.29
Standard Deviation of Differences: 1.01
Mean Difference: 0.77

Figure 17a. Wind speed comparison (m/s) between the radar profiler and rawinsonde for the 0.1-1.0 km layer.



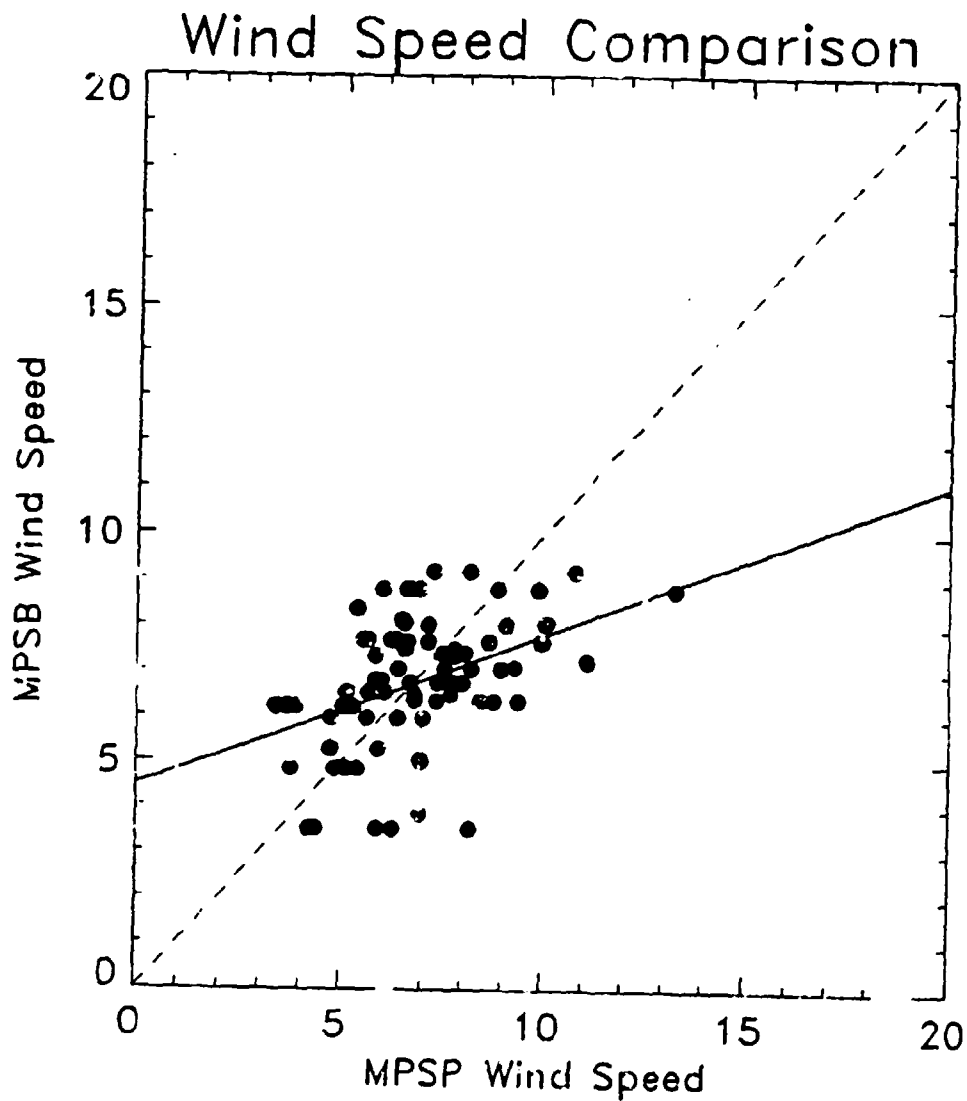
130000, 11 September 1993 to 200000, 11 September 1993
 Los Angeles, CA
 Number of Points = 184
 Height Range (km-AGL): 1.00 - 2.00
 LSF: Slope = 0.26 Intercept = 1.65
 Standard Deviation of Differences: 2.11
 Mean Difference: -1.64

Figure 17b. Wind speed comparison (m/s) between the radar profiler and rawinsonde for the 1.0-2.0 km layer.



130000, 11 September 1993 to 200000, 11 September 1993
Los Angeles, CA
Number of Points = 123
Height Range (km-AGL): 2.00 - 3.00
LSF: Slope = 0.01 Intercept = 3.55
Standard Deviation of Differences: 1.38
Mean Difference: -3.25

Figure 1 c. Wind speed comparison (m/s) between the radar profiler and rawinsonde for the 2.0-3.0 km layer.



130000, 11 September 1993 to 200000, 11 September 1993
 Los Angeles, CA
 Number of Points = 86
 Height Range (km-AGL): 3.00 - 4.00
 LSF: Slope = 0.33 Intercept = 4.48
 Standard Deviation of Differences: 1.77
 Mean Difference: -0.10

Figure 17d. Wind speed comparison (m/s) between the radar profiler and rawinsonde for the 3.0-4.0 km layer.

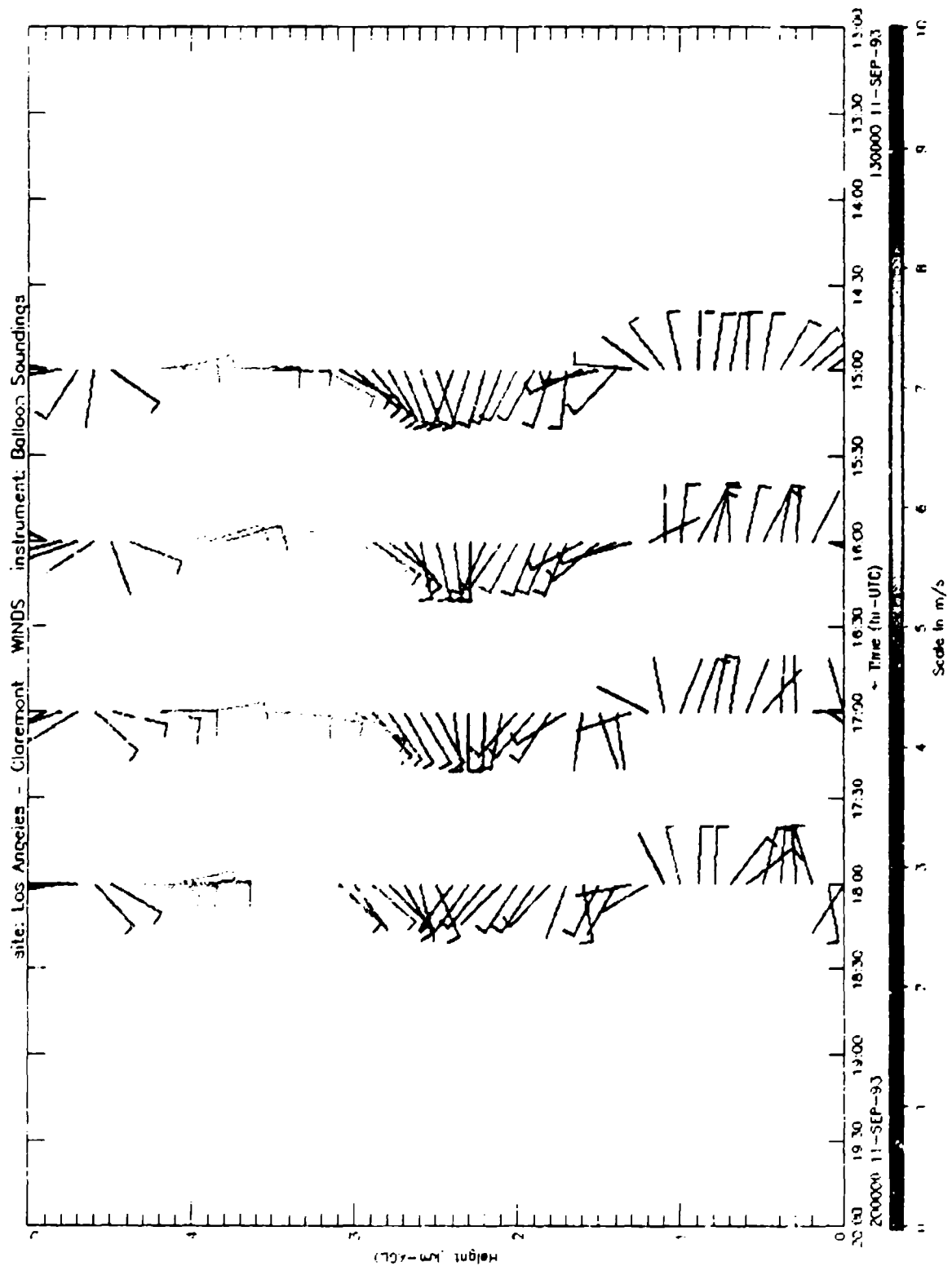
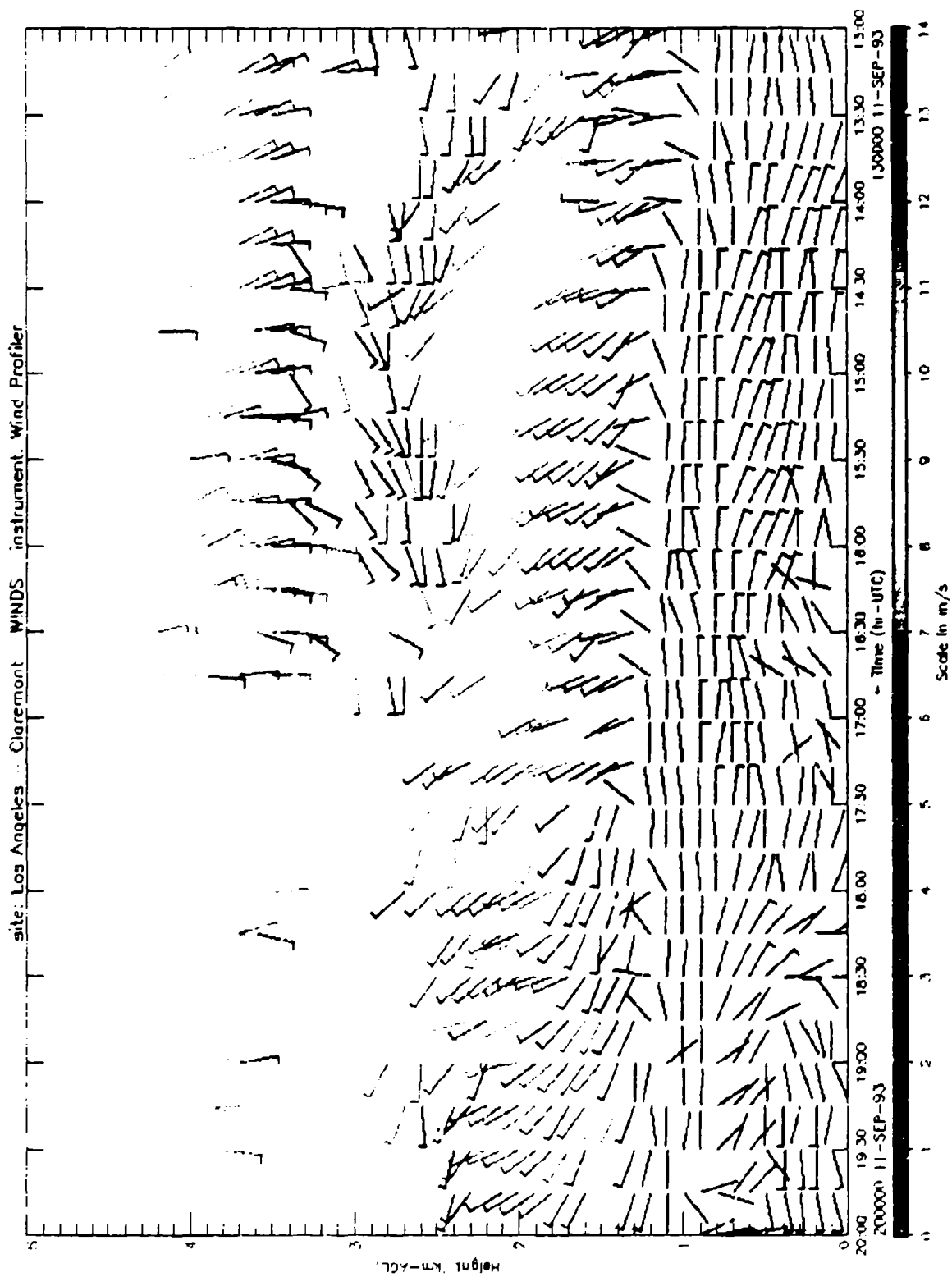


Figure 18. Graphical time-height display of wind velocity from rawinsonde measurements for the period of 1300-2000 UT, 11 September 1993.



45 Figure 19. Graphical time-height display of wind velocity from radar profiler measurements for the period of figure 16.

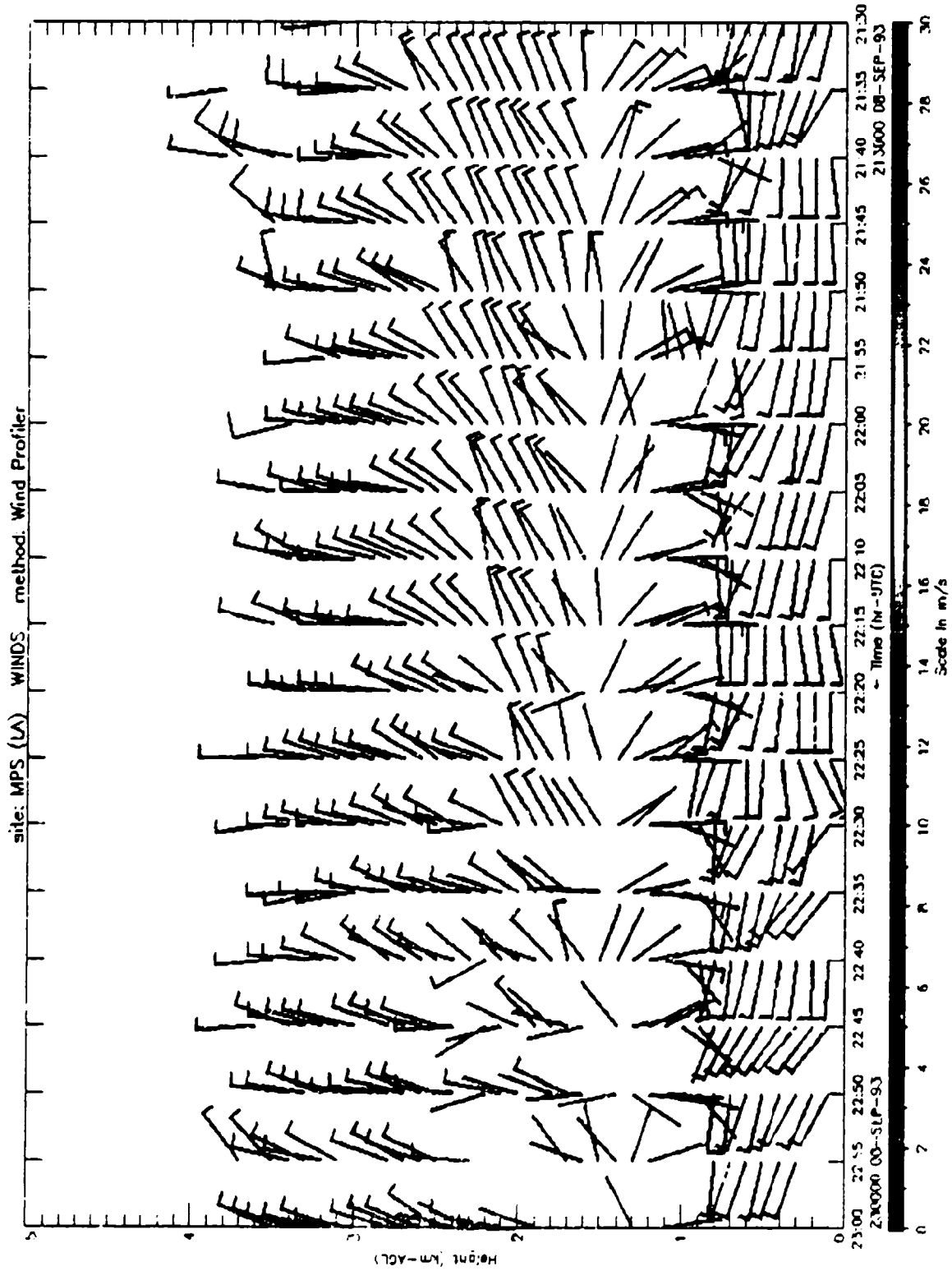


Figure 20. Graphical time-height display of wind velocity from the radar profiler. Five-min averages are displayed every 5 min during 2130-2300 UT, 8 September 1993.

The weak radar return problem may be solved by using well-engineered antennas and receiving sets to improve the signal to noise ratio. As a result, the gap in the wind data should be significantly reduced. Another way to improve the signal to noise ratio might be to increase the power-aperture product; the tradeoff is a larger antenna or higher power. The current peak power of approximately 500 W could be increased to as much as 5 kW without the need for nonstandard components. A larger antenna would reduce portability, unless a somewhat more complicated approach is used, such as folding or assembly of separate panels. Another approach to resolve the problem and increase maximum height of useful return, involves the use of a lower frequency (449 MHz). This approach also requires a somewhat larger antenna, thereby reducing portability. The replacement of the current radar with a newer, better engineered one with increased power should improve performance without significant disadvantages.

Cogan [12] and Miers et al. [4] note potential errors in wind velocities derived from satellite sounding temperatures. The current method of using geostrophic wind may result in errors of 4 to 14 ms^{-1} under common atmospheric conditions and is considered invalid between approximately 15 °N and 15 °S latitude. Research by ARL may reduce these errors by upgrading the merging algorithms and using artificial intelligence techniques (neural networks). A large improvement in the accuracy of wind velocity from satellites must await the advent of active satellite sounders such as a space-based lidar system. An active satellite system also would eliminate the problem of no wind data near the equator. Satellite winds obtained by cloud tracking generally are not useful for the purpose of the MPS. A potential interim solution could use an upgraded rawinsonde to provide data for altitudes above the highest level of the radar profiler. At altitudes well above the boundary layer, changes in mean wind velocities usually are smaller over short periods (1 or 2 hr) except under certain atmospheric conditions such as in the immediate vicinity of fronts. A rawinsonde using the Global Positioning System (GPS) could provide the needed wind velocities at those heights. Adjustments to the rawinsonde data, using a method similar to that employed with satellite data, could account for some of the temporal change during the time between rawinsonde launches. A rawinsonde facility need not be located at every profiler site in a division area. An additional benefit of an interim system is that the gap in available upper wind data near the equator would vanish.

7. Conclusions

The MPS is a mobile system that combines the capabilities of several types of sensing systems to provide atmospheric soundings with a rapid refresh rate that greatly reduces error caused by time staleness. The TD MPS, when fielded, will provide timely atmospheric profiles for fire support and a variety of other Army applications. Examples include biological and chemical defense and support to air mobile operations. It will allow the Integrated Meteorological System (IMETS) to rapidly update models, analyses, and forecasts. Use of a product improvement or phased approach to development and fielding allows this technology to assist the Army without waiting for the final objective system (initial use of interim systems).

The MPS is a true dual use system. The data provided by the TD MPS and later versions will have a variety of applications in the civilian sector. In a similar manner to the related military application, the MPS can provide timely support for airfield operations, giving nearly real time indications of hazardous wind conditions. The ability to generate a picture of very short term flow and virtual temperature patterns can lead to a better understanding of the atmosphere and better modeling at smaller scales. As the Los Angeles experiment showed, this type of system can be invaluable for pollution studies.

The MPS will be a vital part of the data gathering capability for the Owning the Weather concept of operations. In this way it will contribute to making the Army ready to meet the challenges of the coming century.

References

1. Blanco, A., and J. Cogan, 1993: Mobile profiler system improvements to the met error contribution of the artillery error budget. *Proceedings of the 1993 Battlefield Atmospheric Conference*, Las Cruces, NM (in press).
2. Seagraves, M. A., and R. McPeck, 1993: The mobile profiler system: replacing balloon-borne meteorological systems. *Proceedings of the Cloud Impacts on DOD Operations and Systems 1993 Conference*, Ft. Belvoir, VA (in press).
3. Cogan, J. 1992: Battlefield atmospheric soundings in near real time using satellite and ground based remotely sensed data. *Second Battlefield Atmospheric Conference*, sponsored by U.S. Army Research Laboratory, Battlefield Environment Directorate, White Sands Missile Range, NM 88002, 101-110.
4. Miers, B., J. Cogan, and R. Szymber, 1992: *A Review of Selected Remote Sensor Measurements of Temperature, Wind, and Moisture, and Comparison to Rawinsonde Measurements*. ASL-TR-0315, U.S. Army Atmospheric Sciences Laboratory, White Sands Missile Range, NM 88002.
5. Hassel, N., and E. Hudson, 1989: The wind profiler for the NOAA demonstration network. Instruments and observing methods rep. no. 35. *Fourth WMO Technical Conference on Instruments and Methods of Observation (TE-CIMO-IV)*, Brussels, WMO/TD, 261-266.
6. Strauch, R. G., D. A. Merritt, K. P. Moran, K. B. Earnshaw, and D. C. Welsh, 1984: The Colorado wind profiling network. *J. Atmos. Oceanic Technol.*, 1, 37-49.
7. Cogan, J. 1990: *A Technique for Computation of Meteorological Variable Profiles for User Defined Heights and Layers*. ASL-TMR-0005, U.S. Army Atmospheric Sciences Laboratory, White Sands Missile Range, NM 88002.

8. Strauch, R. G., B. L. Weber, A. S. Frisch, C. G. Little, D. A. Merritt, K. P. Moran, and D. C. Welsh, 1987, The precision and relative accuracy of profiler wind measurements. *J. Atmos. Oceanic Technol.*, 4, 563-571.
9. Lawrence, T. R., B. L. Weber, M. J. Post, R. M. Hardesty, R. A. Richter, N. L. Abshire, and F. F. Hall Jr., 1986: *A Comparison of Doppler Lidar, Rawinsonde, and 915 MHz UHF Wind Profiler Measurements of Tropospheric Winds*. NOAA Tech. Memo., ERL WPL-130.
10. Weber, B. L., and D. B. Weurtz, 1990: Comparisons of rawinsonde and wind profiler measurements. *J. Atmos. Oceanic Technol.*, 7, 157-174.
11. Fisher, E. E., F. Brousaides, E. Keppel, F. J. Schidlin, H. C. Herring, and D. Tolzene, 1987: *Meteorological Data Error Estimates*. Document 353-87, Meteorology Group, Range Commanders Council, White Sands Missile Range, NM 88002.
12. Cogan, J. 1993: *Some Potential Errors in Satellite Wind Estimates Using the Geostrophic Approximation and the Thermal Wind*. Technical Memorandum Report ARL-MR-36, Battlefield Environment Directorate, U. S. Army Research Laboratory, White Sands Missile Range, NM 88002.

Acronyms and Abbreviations

ARL	Army Research Laboratory
AWS	Air Weather Service
BED	Battlefield Environment Directorate
CAAM	Computer Assisted Artillery Meteorology
CLASS	Cross-chain Loran Atmospheric Sounding System
ETL	Environmental Technology Laboratory
GPS	Global Positioning System
IMETS	Integrated Meteorological System
MDS	Meteorological Data System
MET	meteorological
MET-CM	computer meteorological message
mmd	magnitude of the mean difference
MPS	Mobile Profiler System
MPSB	Mobile Profiler System Balloon
NOAA	National Oceanic and Atmospheric Administration
NWS	National Weather Service
PDT	Pacific daylight time
PM-EW/RSTA	Project Manager, Electronic Warfare/Reconnaissance Surveillance and Target Acquisition
RASS	Radio Acoustic Sounding System

TD	Technical Demonstration
UT	Universal Time
WMO	World Meteorological Organization
WSMR	White Sands Missile Range

Distribution

DISTRIBUTION

	Copies
Commandant U.S. Army Chemical School ATTN: ATZN-CM-CC (Mr. Barnes) Fort McClellan, AL 36205-5020	1
NASA Marshal Space Flight Center Deputy Director Space Science Laboratory Atmospheric Sciences Division ATTN: E501 (Dr. Fichtl) Huntsville, AL 35802	1
NASA/Marshall Space Flight Center Atmospheric Sciences Division ATTN: Code ED-41 Huntsville, AL 35812	1
Deputy Commander U.S. Army Strategic Defense Command ATTN: CSSD-SL-L (Dr. Lilly) P.O. Box 1500 Huntsville, AL 35807-3801	1
Deputy Commander U.S. Army Missile Command ATTN: AMSMI-RD-AC-AD (Dr. Peterson) Redstone Arsenal, AL 35898-5242	1
Commander U.S. Army Missile Command ATTN: AMSMI-RD-DE-SE (Mr. Lill, Jr.) Redstone Arsenal, AL 35898-5245	1
Commander U.S. Army Missile Command ATTN: AMSMI-RD-AS-SS (Mr. Anderson) Redstone Arsenal, AL 35898-5253	1
Commander U.S. Army Missile Command ATTN: AMSMI-RD-AS-SS (Mr. B. Williams) Redstone Arsenal, AL 35898-5253	1
Commander U.S. Army Missile Command Redstone Scientific Information Center ATTN: AMSMI-RD-CS-R/Documents Redstone Arsenal, AL 35898-5241	1

Commander
 U.S. Army Aviation Center
 ATTN: ATZQ-D-MA (Mr. Heath) 1
 Fort Rucker, AL 36362

Commander
 U.S. Army Intelligence Center
 and Fort Huachuca
 ATTN: ATSI-CDC-C (Mr. Colanto) 1
 Fort Huachuca, AZ 85613-7000

Northrup Corporation
 Electronics Systems Division
 ATTN: Dr. Tooley 1
 2301 West 120th Street, Box 5032
 Hawthorne, CA 90251-5032

Commander
 Pacific Missile Test Center
 Geophysics Division
 ATTN: Code 3250 (Mr. Battalino) 1
 Point Mugu, CA 93042-5000

Commander
 Code 3331
 Naval Weapons Center
 ATTN: Dr. Shlanta 1
 China Lake, CA 93555

Lockheed Missiles & Space Co., Inc.
 Kenneth R. Hardy
 ORG/91-01 B/255 1
 3251 Hanover Street
 Palo Alto, CA 94304-1191

Commander
 Naval Ocean Systems Center
 ATTN: Code 54 (Dr. Richter) 1
 San Diego, CA 92152-5000

Meteorologist in Charge
 Kwajalein Missile Range
 P.O. Box 67 1
 APO San Francisco, CA 96555

U.S. Department of Commerce Center
 Mountain Administration
 Support Center, Library, R-51
 Technical Reports
 325 S. Broadway 1
 Boulder, CO 80303

Dr. Hans J. Liebe NTIA/ITS S 3 325 S. Broadway Boulder, CO 80303	1
NCAR Library Serials National Center for Atmos Research P.O. Box 3060 Boulder, CO 80307-3000	1
Headquarters Department of the Army ATTN: DAMI-POI Washington, DC 20310-1067	1
Mil Asst for Env Sci Ofc of the Undersecretary of Defense for Rsch & Engr/R&AT/E&LS Pentagon - Room 3D129 Washington, DC 20301-3030	1
Headquarters Department of the Army DEAN-RMD/Dr. Gomez Washington DC 20314	1
Director Division of Atmospheric Science National Science Foundation ATTN: Dr. Pierly 1800 G. Street, N.W. Washington, DC 20550	1
Commander Space & Naval Warfare System Command ATTN: PMW-145-1G Washington, DC 20362-5100	1
Director Naval Research Laboratory ATTN: Code 4110 (Mr. Ruhnke) Washington, DC 20375-5000	1
Commandant U S. Army Infantry ATTN: ATSH-CD-CS-OR (Dr. E. Dutoit) Fort Benning, GA 30905-5090	1
USAFETAC/DNE Scott AFB, IL 62225	1

Air Weather Service Technical Library - FL4414 Scott AFB, IL 62225-5458	1
USAFETAC/DNE ATTN: Mr. Glauber Scott AFB, IL 62225-5008	1
Headquarters AWS/DOO Scott AFB, IL 62225-5008	1
Commander U.S. Army Combined Arms Combat ATTN: ATZL-CAW Fort Leavenworth, KS 66027-5300	1
Commander U.S. Army Space Institute ATTN: ATZI-SI Fort Leavenworth, KS 66027-5300	1
Commander U.S. Army Space Institute ATTN: ATZL-SI-D Fort Leavenworth, KS 66027-7300	1
Commander Phillips Lab ATTN: PL/LYP (Mr. Chisholm) Hanscom AFB, MA 01731-5000	1
Director Atmospheric Sciences Division Geophysics Directorate Phillips Lab ATTN: Dr. McClatchey Hanscom AFB, MA 01731-5000	1
Raytheon Company Dr. Sonnenschein Equipment Division 528 Boston Post Road Sudbury, MA 01776 Mail Stop 1K9	1
Director U.S. Army Materiel Systems Analysis Activity ATTN: AMXSU-CR (Mr. Marchetti) Aberdeen Proving Ground, MD 21005-5071	1

Director
U.S. Army Materiel Systems Analysis Activity
ATTN: AMXSY-MP (Mr. Cohen) 1
Aberdeen Proving Ground, MD 21005-5071

Director
U.S. Army Materiel Systems Analysis Activity
ATTN: AMXSY-AT (Mr. Campbell) 1
Aberdeen Proving Ground, MD 21005-5071

Director
U.S. Army Materiel Systems
Analysis Activity
ATTN: AMXSY-CS (Mr. Bradley) 1
Aberdeen Proving Ground, MD 21005-5071

Director
ARL Chemical Biology
Nuclear Effects Division
ATTN: AMSRL-SL-CO 1
Aberdeen Proving Ground, MD 21010-5423

Army Research Laboratory
ATTN: AMSRL-D 1
2800 Powder Mill Road
Adelphi, MD 20783-1145

Army Research Laboratory
ATTN: AMSRL-OP-SD-TP 1
Technical Publishing
2800 Powder Mill Road
Adelphi, MD 20783-1145

Army Research Laboratory
ATTN: AMSRL-OP-CI-SD-TL 1
2800 Powder Mill Road
Adelphi, MD 20783-1145

Army Research laboratory
ATTN: AMSRL-SS-SH 1
(Dr. Sztankay)
2800 Powder Mill Road
Adelphi, MD 20783-1145

U.S. Army Space Technology
and Research Office
ATTN: Ms. Brathwaite 1
5321 Riggs Road
Gaithersburg, MD 20882

National Security Agency
ATTN: W21 (Dr. Longbothum) 1
9800 Savage Road
Fort George G. Meade, MD 20755-6000

OIC-NAVSWC
Technical Library (Code E-232) 1
Silver Springs, MD 20903-5000

Commander
U.S. Army Research office
ATTN: DRXRO-GS (Dr. Flood) 1
P.O. Box 12211
Research Triangle Park, NC 27009

Dr. Jerry Davis
North Carolina State University
Department of Marine, Earth, and
Atmospheric Sciences 1
P.O. Box 8208
Raleigh, NC 27650-8208

Commander
U.S. Army CECRL
ATTN: CECRL-RG (Dr. Boyne) 1
Hanover, NH 03755-1290

Commanding Officer
U.S. Army ARDEC
ATTN: GMCAR-IMI-I, Bldg 59 1
Dover, NJ 07806-5000

Commander
U.S. Army Satellite Comm Agency
ATTN: DRCPM-SC-3 1
Fort Monmouth, NJ 07703-5303

Commander
U.S. Army Communications-Electronics
Center for EW/RSTA
ATTN: AMSEL-EW-MD 1
Fort Monmouth, NJ 07703-5303

Commander
U.S. Army Communications-Electronics
Center for EW/RSTA
ATTN: AMSEL-EW-D 1
Fort Monmouth, NJ 07703-5303

Commander
 U.S. Army Communications-Electronics
 Center for EW/RSTA
 ATTN: AMSEL-RD-EW-SP 1
 Fort Monmouth, NJ 07703-5206

Commander
 Department of the Air Force
 OL/A 2d Weather Squadron (MAC) 1
 Holloman AFB, NM 88330-5000

PL/WE 1
 Kirtland AFB, NM 87118-6008

Director
 U.S. Army TRADOC Analysis Center
 ATTN: ATRC-WSS-R 1
 White Sands Missile Range, NM 88002-5502

Director
 U.S. Army White Sands Missile Range
 Technical Library Branch
 ATTN: STEWS-IM-IT 3
 White Sands Missile Range, NM 88002

Army Research Laboratory
 ATTN: AMSRL-BE (Mr. Veazy) 1
 Battlefield Environment Directorate
 White Sands Missile Range, NM 88002-5501

Army Research Laboratory
 ATTN: AMSRL-BE-A (Mr. Rubio) 1
 Battlefield Environment Directorate
 White Sands Missile Range, NM 88002-5501

Army Research Laboratory
 ATTN: AMSRL-BE-M (Dr. Niles) 1
 Battlefield Environment Directorate
 White Sands Missile Range, NM 88002-5501

Army Research Laboratory
 ATTN: AMSRL-BE-W (Dr. Seagraves) 1
 Battlefield Environment Directorate
 White Sands Missile Range, NM 88002-5501

USAF Rome Laboratory Technical
 Library, FL2810 1
 Corridor W. STE 262, PL/SUL
 26 Electronics Parkway, Bldg 106
 Griffiss AFB, NY 13441-4514

AFMC/DOW 1
 Wright-Patterson AFB, OH 03340-5000

Commandant
 U.S. Army Field Artillery School
 ATTN: ATSF-TSM-TA (Mr. Taylor) 1
 Fort Sill, OK 73503-5600

Commander
 U.S. Army Field Artillery School
 ATTN: ATSF-F-FD (Mr. Gullion) 1
 Fort Sill, OK 73503-5600

Commander
 Naval Air Development Center
 ATTN: Al Salik (Code 5012) 1
 Warminster, PA 18974

Commander
 U.S. Army Dugway Proving Ground
 ATTN: STEDP-MT-M (Mr. Bowers) 1
 Dugway, UT 84022-5000

Commander
 U.S. Army Dugway Proving Ground
 ATTN: STEDP-MT-DA-L 1
 Dugway, UT 84022-5000

Defense Technical Information Center
 ATTN: DTIC-OCF 2
 Cameron Station
 Alexandria, VA 22314-6145

Commander
 U.S. Army OEC
 ATTN: CSTE-EFS 1
 Park Center IV
 4501 Ford Ave
 Alexandria, VA 22302-1458

Commanding Officer
 U.S. Army Foreign Science & Technology Center
 ATTN: CM 1
 220 7th Street, NE
 Charlottesville, VA 22901-5396

Naval Surface Weapons Center
 Code G63 1
 Dahlgren, VA 22448-5000

Commander and Director
 U.S. Army Corps of Engineers
 Engineer Topographics Laboratory
 ATTN: ETL-GS-LB 1
 Fort Belvoir, VA 22060

U.S. Army Topo Engineering Center ATTN: CETEC-ZC Fort Belvoir, VA 22060-5546	1
Commander USATRADO ATTN: ATCD-FA Fort Monroe, VA 23651-5170	1
TAC/DOWP Langley AFB, VA 23665-5524	1
Commander Logistics Center ATTN: ATCL-CE Fort Lee, VA 23801-6000	1
Science and Technology 101 Research Drive Hampton, VA 23666-1340	1
Commander U.S. Army Nuclear and Chemical Agency ATTN: MONA-2B, Bldg 2073 Springfield, VA 22150-3198	1
Record Copy	3
Total	89

**END
FILMED**

DATE:
10-94

DTIC